BATTELLE MEMORIAL INSTITUTE

COLUMBUS LABORATORIES • 505 KING AVENUE • COLUMBUS, OHIO 43201

DEDICATED TO THE ADVANCEMENT OF SCIENCE

[redacted]

FIELDS OF RESEARCH

Aeronautics — Astronautic
Agricultural Chemistry
Agricultural Economics
Alloy Development
Applied Mathematics
Area Economics
Biochemistry
Biophysics — Bionics
Catalysis — Surface Chemistry
Ceramics
Chemical Engineering
Chemical Processes
Communications Science
Computer Technology
Corrosion Technology
Earth — Atmospheric Sciences
Electrochemistry
Electronics
Energy Conversion
Engineering — Structural Materials
Environmental Systems
Extractive Metallurgy
Extreme-Temperature Technology
Ferrous Metallurgy
Food Technology
Foundry Practice
Fuels — Combustion
Glass Technology
Graphic Arts Technology
Immunology — Cancer Studies
Industrial Economics
Industrial Physics
Information Research
Inorganic Chemistry
Instrumentation
Light Alloys — Rare Metals
Lubricant Technology
Materials Separation — Concentration
Mechanical Engineering
Metal Fabrication Engineering
Metal Finishing
Metallurgical Processes
Microbiology
Microscopy — Mineralogy
Nondestructive Evaluation Technology
Nonferrous Metallurgy
Nucleonics
Ocean Engineering
Organic Chemistry
Organic Coatings
Packaging Research
Particle Dynamics
Petrochemicals
Petroleum Engineering
Pharmaceutical Chemistry
Physical Chemistry
Production Engineering
Psychological Sciences
Pulp — Paper Technology
Radioisotopes — Radiation
Reactor Technology
Refractories
Reliability Engineering
Rubber — Plastics
Semiconductors — Solid-State Devices
Sound — Vibration
Systems Engineering
Textiles — Fibers
Theoretical — Applied Mechanics
Thermodynamics
Transportation
Welding — Metals-Joining Technology
Wood — Forest Products

REPORT NUMBER

BMI-NLVP-FTR-65-1

GRAVITY-ASSISTED TRAJECTORIES FOR UNMANNED SPACE EXPLORATION

to

NATIONAL AERONAUTICS AND SPACE ADMINISTRATION

September 23, 1965

CONTRACT NUMBER NASw-1146

by

R. F. Porter, R. G. Luce, and D. S. Edgecombe

R. F. Porter - Author

R. G. Luce - Author

D. S. Edgecombe - Author

B. W. Davis

Approved by: B. W. Davis
Director
NASA Launch Vehicle Planning Project

BATTELLE MEMORIAL INSTITUTE
505 King Avenue
Columbus, Ohio 43201

TABLE OF CONTENTS

FIGURES

TABLE OF CONTENTS (Continued)

ABSTRACT

13067

The concept of utilizing a close encounter with another planet to modify the heliocentric trajectories of unmanned space probes has been examined. This study consisted of both a literature survey and original analytical work. The potential advantages of swingbys of Venus and Jupiter are illustrated for three classes of missions: (1) probes to the outer reaches of the solar system, (2) probes to the near vicinity or impact with the Sun, and (3) probes out of the ecliptic plane.

GRAVITY-ASSISTED TRAJECTORIES FOR UNMANNED SPACE EXPLORATION

by

R. F. Porter, R. G. Luce, and D. S. Edgecombe

INTRODUCTION

The objectives of the study covered in this report were to examine the role of gravity-assisted trajectories in unmanned space exploration, to delineate the classes of missions which may benefit most significantly from planet swingby techniques, to indicate the effect of gravity-assisted trajectories upon launch-vehicle performance requirements, and to suggest avenues of further study.

The concept of utilizing a close planetary encounter for the purpose of modifying the heliocentric orbit of a spacecraft is not new, having been studied by Hohmann in 1928 for an Earth-Mars-Venus-Mercury voyage. More recently, many researchers have investigated the technique in varying degrees of detail and many significant papers have appeared in the technical literature. A bibliography of these papers is presented in Appendix A.

Almost all of the papers on this topic are concerned with missions in the Mercury-Venus-Earth-Mars regime, with a swingby of one or more of these planets being utilized to reduce the energy requirements for probes to other planets or to the vicinity of the Sun. Notable exceptions are the well-known paper by Hunter (Reference 1), wherein swingby of Jupiter is suggested to reduce the launch-energy requirements for the more strenuous missions needed for solar system exploration, and the more recent work of Niehoff (Reference 2). In the latter report, a quantitative treatment of Jupiter-assisted trajectories appears, although these trajectories are restricted to the plane of the ecliptic.

An examination of the work done on this subject reveals that Jupiter represents the most dramatic potential for unmanned probes. For this reason, a major portion of the present effort is devoted to an analysis of Jupiter-assisted trajectories.

SCOPE

This study has been performed from the point of view of the launch-vehicle planner, as a step in determining what the impact of gravity-assisted trajectories might be on launch-vehicle requirements for one-way unmanned missions. Toward this end, the launch-energy savings have been of paramount interest, although it is not possible to completely avoid some rudimentary consideration of flight times, guidance requirements, and communication distances even for a preliminary study of this nature. Nevertheless, the guiding philosophy has been that the use of a gravity-assisted trajectory is invariably a complicating mission factor and that serious consideration of this technique should be reserved for those missions which will reap the most significant performance benefits. The delineation of these missions is thus a critical first step in assessing the impact of gravity-assisted trajectories.

To benefit from the conclusions of other researchers in this field, a literature survey was conducted. It became apparent from this survey that Jupiter holds great promise as a swingby target for some of the more difficult unmanned missions (Reference 1), but there is a paucity of quantitative general information on Jupiter-assisted trajectories.*

The analytical phase of this investigation was concerned almost exclusively with Jupiter-assisted trajectories, since the use of the near

---

* Reference 2 contains a great deal of information on this subject, but it was not known to the authors at the time.

planets appeared to be treated adequately in the literature. Three types of Jupiter-assisted trajectories were analyzed. Specifically, the Jupiter swingby technique was examined as an assist to probe the outer reaches of the solar system, to provide drastic perihelion reduction for solar probes, and to deflect heliocentric orbits out of the ecliptic plane.

For the first class of missions, those to distant areas, the time of flight becomes a dominating constraint for several reasons. As a consequence, a specific objective of the analysis was to determine those trajectories that minimize the total flight time to a prescribed solar radial distance for a given Earth launch velocity.

For the second class of missions, the solar probes, those trajectories that minimize perihelion for a given Earth launch velocity have been examined and compared with direct Earth launch, from both energy and time-of-flight standpoints. For those Earth launch velocities which enable actual impact with the Sun to occur, the trade-off between Earth launch velocity and total time of flight was determined.

For the third class of missions, wherein final trajectories which lie out of the plane of the ecliptic are considered, two types of trajectories were studied. These were trajectories which pass directly over the Sun, being inclined 90° to the ecliptic plane, and those which maximize the obtainable velocity component normal to the ecliptic plane, after Jupiter encounter, for a given Earth launch velocity.

It must be emphasized that this study has been primarily concerned with a survey of the performance benefits to be gained by gravity-assisted trajectories, and no detailed consideration has been given to guidance requirements, communication distances, antenna pointing angles in relation to the Sun, etc. Some of the references cited do contain a few data on these other parameters. These considerations cannot be adequately treated unless the

analysis is restricted to a very specific mission, and obviously no attempt has been made to do so in this report. Consequently, the use of Earth launch velocity as the only criterion for comparing a gravity-assisted trajectory with a direct flight can be quite misleading. In general, this study must be considered only as an attempt to identify those unmanned exploration missions for which the gravity-assist mode shows sufficient promise for more detailed study by mission planners.

APPROACH AND ASSUMPTIONS

For the analytical portion of this study, a digital computer program was written in Fortran IV for the CDC-3400 computer. A discussion of the computational procedure may be found in Appendix B.

The following principal assumptions were made:

(1) The patched-conic-trajectory technique is applicable; that is, the spacecraft is under the influence of only one attracting body at a time.

(2) Both the Earth and Jupiter are in circular co-planar orbits.

(3) All Earth launches make maximum use of the Earth's orbital speed around the Sun by aligning the outgoing asymptote of the Earth-escape hyperbola with the direction of the Earth's motion.

(4) Except for those orbits specifically perturbed out of the ecliptic plane, all heliocentric orbits lie in the ecliptic plane.

(5) Both the Earth and Jupiter are assumed to have a sphere of influence of zero radius (see Appendix B).

All launch energy requirements are expressed in terms of the characteristic velocity, V_C, required at a reference altitude of 100 nautical miles above the Earth's surface.

RESULTS OF THE STUDY

The following discussion of the results of the study is divided into five parts: (1) utilization of Venus and Mars gravitational fields, (2) Jupiter-gravity assist for deep solar system probes, (3) Jupiter-assisted mission to Saturn, (4) Jupiter-assisted solar probes, and (5) out-of-the-ecliptic missions using Jupiter assist.

Utilization of Venus and Mars Gravitational Fields

The employment of gravity-assisted trajectories utilizing the two planets closest to Earth has been examined extensively by other authors. Many of these studies have been concerned with manned missions, the swingby mode being used to reduce Earth re-entry velocity, lengthen stay times, or widen launch opportunity windows in the face of launch-energy constraints. References 3, 4, 5, 6, 7, and 8 are in this general category. Of more immediate interest for this study, however, are those investigations which utilize the gravitational fields of Venus or Mars for unmanned probes.

In Reference 9, Casal and Ross examined possible solar probe missions employing single or multiple Venus swingbys. In addition to discussing the advantages of such an approach and the mechanics of achieving it, attention is given to such details as spacecraft configuration, power source, thermal protection, attitude control, and the guidance problem. The authors noted that the benefits to be gained include a closer solar approach than obtainable by direct flight, an opportunity to conduct one or two Venusian

inspections while enroute, and a general reduction in propulsion requirements. To obtain these benefits, they propose the use of a guidance and propulsion system capable of five in-course corrections: (1) Earth departure, (2) first Venusian approach, (3) first Venusian departure, (4) solar perihelion, and (5) second Venusian encounter. Casal and Ross conclude that a single swingby of Venus is superior to direct flight for perihelia in the 0.3 to 0.4 a.u. range, while perihelion distances as small as 0.2 a.u. appear possible with substantial payload weights for double-swingby trajectories if sustained and reliable spacecraft operation for periods of 1½ to 2½ years is obtainable.

Perhaps the most detailed analysis of a gravity-assisted mission to be found in the literature is contained in Reference 10. Here, Sturms and Cutting have examined, in detail, one of the missions suggested by Minovitch in Reference 11, a 1970 mission to Mercury using a Venus swingby. Special attention is given to the question of guidance requirements. The authors conclude that the required guidance accuracy, while more stringent than for current planetary missions, is within the state of the art of current Earth-based radio-command systems if the vehicle is capable of performing three in-course corrections--one after Earth launch, one prior to Venusian encounter, and one after departing from Venus. As a result of the Venus encounter, the characteristic velocity required for the mission is about 38,300 feet per second, as compared with about 42,600 feet per second for the direct flight to Mercury at that time. It may be observed that the direct flight in this time period would require at least an SLV3X-Centaur-Kick launch vehicle; whereas Sturms and Cutting point out that the Atlas-Centaur can deliver over 1300 pounds for the indirect flight they suggest.

The literature survey and the results of additional analytical work performed as part of this investigation indicate that Mars does not seem to be particularly useful for gravity-assisted trajectories for unmanned probes.

This is primarily a consequence of its small mass and the relatively large synodic period (780 days) as compared with those of the other planets. In Reference 2, Niehoff examines an Earth-Mars-Jupiter mission and concludes that while there is some performance advantage over the direct flight to Jupiter, the opportunities for such a mission are few, the next one appearing in 1984. The further conclusion is reached that the moderate launch-energy reductions made possible by the Mars swingby do not seem to justify the added mission complexity. The direct flight is recommended.

Jupiter-Gravity Assist for Deep Solar System Probes

As mentioned previously, Jupiter seems to hold the most dramatic promise for gravity-assisted missions because of its enormous mass and because its synodic period is relatively small, about 13 months.

Figure 1 illustrates the relationship between Earth launch characteristic velocity and the total minimum flight time to reach a desired radial distance from the Sun, for trajectories using Jupiter-gravity assist. The procedure for computing these data is outlined in Appendix B, and consists of selecting a miss distance at Jupiter which modifies the heliocentric trajectory of the spacecraft so as to minimize the total time for each radial distance and V_C combination. In no case was the distance of closest approach to Jupiter permitted to be less than 1.5 planet radii. This is an arbitrary minimum which is probably conservative from the standpoint of risk of encountering the Jovian atmosphere.

Although a consideration of guidance requirements is beyond the scope of this paper, it should be noted that the flight times were usually rather insensitive to variations in Jupiter miss distance. For example, a trip to 18 a.u. with V_C = 55,200 ft/sec can be accomplished in a minimum of 1420 days using an aiming point miss distance, d, of about 7.6 Jupiter radii

(see Figure B-2 of Appendix B for illustration of d). If an error of one Jupiter radius is permitted in either direction, the difference in flight time to 18 a.u. is increased only about 20 days.

The mechanical advantages of Jupiter-assisted trajectories can be seen by comparing Figure 1 with Figure 2. In Figure 2, time-of-flight contours are plotted for direct flights from Earth. Two effects are apparent: the minimum launch velocities for probing the outer reaches of the solar system are reduced by Jupiter swingby, and second, use of the Jupiter assist can be elected to reduce either launch-velocity requirements or times of flight, in general.

If the maximum permissible time of flight is a limiting constraint, it is interesting to note the velocity savings which can be obtained for a fixed flight time. This is shown in Figure 3, wherein the difference has been computed between the velocity required for direct flight and that required to obtain the same total flight time for the Jupiter-swingby mode. This velocity difference may be viewed as an equivalent velocity increment which must be provided either by a propulsion stage or by the Jupiter swingby to achieve the given distance in a given time. For example, if a mission to 17 a.u. is postulated to have a flight-time constraint of 1000 days, the Jupiter assist is seen to be equivalent to about a 7000 ft/sec upper stage.

It may be noted that the velocity savings for all flight times less than 1000 days are very nearly the same; furthermore, these lines terminate near 20 a.u. because this is the limiting distance for direct flights of 1000 days or less using reasonable launch velocities (see Figure 2). Similarly, the lines for the greater flight times have a lower bound which is the least distance reached in the specified time using optimized Jupiter assist.

In Figure 4, a different approach is taken. Here, the launch velocity is a parameter and the flight time savings obtained by Jupiter swingby

are plotted. To provide a convenient reference, contours of constant flight time with Jupiter assist are provided. Interestingly, the greater time savings occur for the lower Earth launch velocities. The dashed portion of this figure is included only to show the trends; a comparison in this region is not valid since flight beyond 11 a.u. is not possible by direct flight with V_C = 50,000 ft/sec.

Jupiter-Assisted Mission to Saturn

In the preceding paragraphs, probes to the outer reaches of the solar system have been studied with no attempt to arrive at a specific planet. A refinement of this idea has been studied by Niehoff (Reference 2), wherein a swingby of Jupiter is used as an assist to reach Saturn. The author examines a mission occuring during a 1977 launch opportunity, but indicates that similar opportunities will occur in 1976 and 1978. Saturn is reached in 1072 days with an Earth-launch characteristic velocity of 50,000 ft/sec. This would mean that a spacecraft weighing well over 1000 pounds could be launched by a Saturn 1B-Centaur vehicle. Although the same mission can be flown directly with a characteristic velocity of about 52,400 ft/sec (see Figure 2), a payload of the same magnitude would require the addition of a kick stage to the Saturn 1B-Centaur vehicle.

The use of Jupiter assist to actually reach planets beyond Saturn has not been explored, but the relative benefits to be obtained may be even greater than for Saturn if the planetary conjunctions permit the realization of the potential energy gains.

Jupiter-Assisted Solar Probes

Figure 5 shows the velocity requirements and trip times for solar probes launched directly from Earth and those using Jupiter assist. As

discussed in Appendix B, passage is in front of Jupiter with a turning angle selected to minimize the final heliocentric velocity of the spacecraft. After encounter, the spacecraft is at the aphelion of a new elliptical orbit with a reduced perihelion.

It can be seen in Figure 5 that perihelion distances closer than about 0.3 a.u. are obtained with smaller launch velocities if the Jupiter-swingby mode is used. An enormous saving for the very close solar probes is apparent, but so is the rather substantial flight-time penalty associated with the circuitous route past Jupiter.

It is possible to reduce significantly the Jupiter-swingby flight times for solar probes, at the expense of Earth-launch velocity. A particular tradeoff of this nature is illustrated in Figure 6 for probes which impact on the Sun. Here, launch velocities greater than 50,000 ft/sec are used to permit the final heliocentric velocity after Jupiter encounter to be directed radially toward the Sun. A flight-time saving is obtained on both the outbound and inbound trajectories. A limitation exists, as shown in the figure, since the combination of turning angle and approach velocity for higher energy trajectories can require passage closer than the adopted minimum of 1.5 Jupiter radii.

Out-of-the-Ecliptic Missions Using Jupiter Assist

The attainment of orbital paths far removed from the plane of the ecliptic is extremely expensive, in terms of launch energy, if only the more obvious direct flights from Earth orbit are considered. Hunter (Reference 1) points out that a launch velocity near 140,000 ft/sec is required to launch directly from Earth 90 degrees out of the ecliptic plane and go over the Sun at a distance of 1 a.u. He suggests that a Jupiter swingby could do as well with an Earth launch velocity of 52,000 ft/sec. Figure 7 verifies this

conclusion and shows the relationship between height out of the ecliptic at Sun passage for two types of swingbys. These types are discussed more fully in Appendix B; but briefly, one swingby is designed to deflect the heliocentric orbit 90 degrees from the ecliptic, while the other deflects the final orbit to a smaller inclination angle, but in such a way as to maximize the component of spacecraft velocity normal to the ecliptic plane. Only the first type of trajectory actually passes directly over the Sun, the second type being inclined at the angles shown in Figure 8. In general, of course, a wide range of inclination angles is obtainable, but only these two types are considered since the primary purpose was to illustrate the power of the Jupiter swingby in producing orbits far removed from the ecliptic plane.

The Type II trajectories always require turning the relative velocity vector 90 degrees during Jupiter swingby, whereas the Type I turning angles are slightly smaller but in a different plane, as discussed in Appendix B. These turning angles are sufficiently large to require passage closer than 1.5 Jupiter radii if Earth launch velocities much beyond 60,000 ft/sec are used. This may be inferred from an inspection of Figure B-2 in Appendix B.

Figure 9 presents the maximum distance from the ecliptic plane reached by these trajectories. It is interesting to note that even a minimum-energy orbit to Jupiter can be deflected to produce a new heliocentric orbit inclined over 23 degrees to the ecliptic plane and reaching almost 2.5 AU above the plane at its highest point. Type I orbits, inclined 90 degrees, are not possible unless the relative approach velocity at Jupiter exceeds Jupiter's orbital speed aroung the Sun. This occurs for slightly over 50,000 ft/sec Earth launch characteristic velocity.

CONCLUSIONS

The results of this study suggest that gravity-assisted trajectories deserve very serious consideration for four types of the more strenuous unmanned missions:

(1) Probes to the planet Mercury

(2) Probes to the near vicinity of the Sun, from 0.4 a.u. to impact

(3) Probes to the outer reaches of the solar system beyond Jupiter, including missions to the outer planets

(4) Probes to regions out of the ecliptic plane.

Mars does not represent sufficient potential to warrant the added complexity of swingby trajectories for unmanned probes. Only swingbys of Venus and Jupiter appear to be useful for these--Venus being utilized for the Mercury probes and solar probes from about 0.4 a.u. to possibly as close as 0.2 a.u., and Jupiter being used for the remainder.

Although the Venus-gravity-assisted solar probes and the missions to Mercury have been analyzed in detail, the Jupiter-assisted missions have not been explored in depth, and a definitive study of each of the suggested Jupiter missions is required to properly weigh the conflicting mission factors such as energy requirements, trip times, spacecraft reliability, guidance problems, antenna pointing angles, communication distances, etc. The inescapable flight through the asteroid belt for Jupiter missions also requires special consideration.

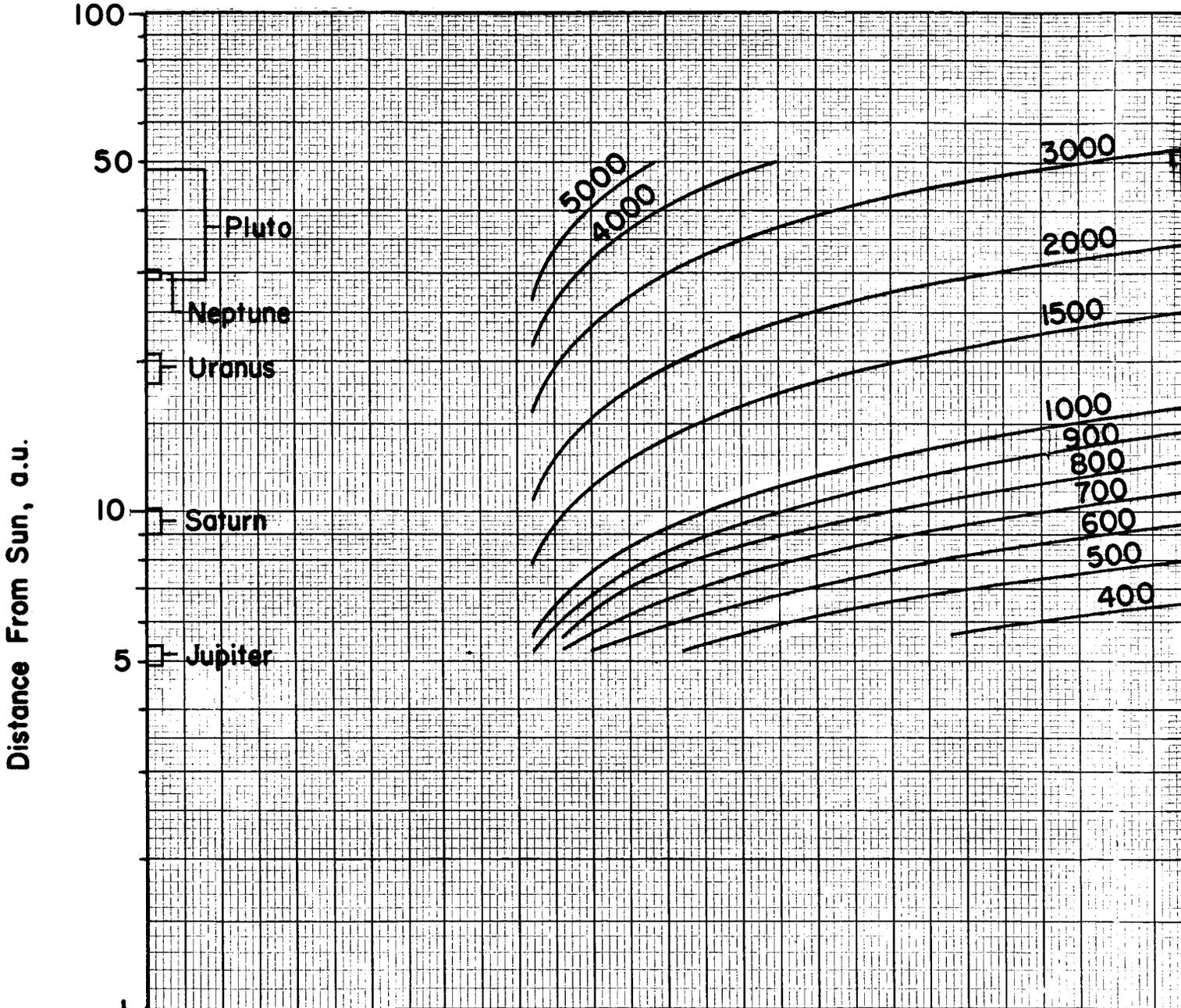

FIGURE I. VELOCITY REQUIRED FOR OUTER PLANETARY

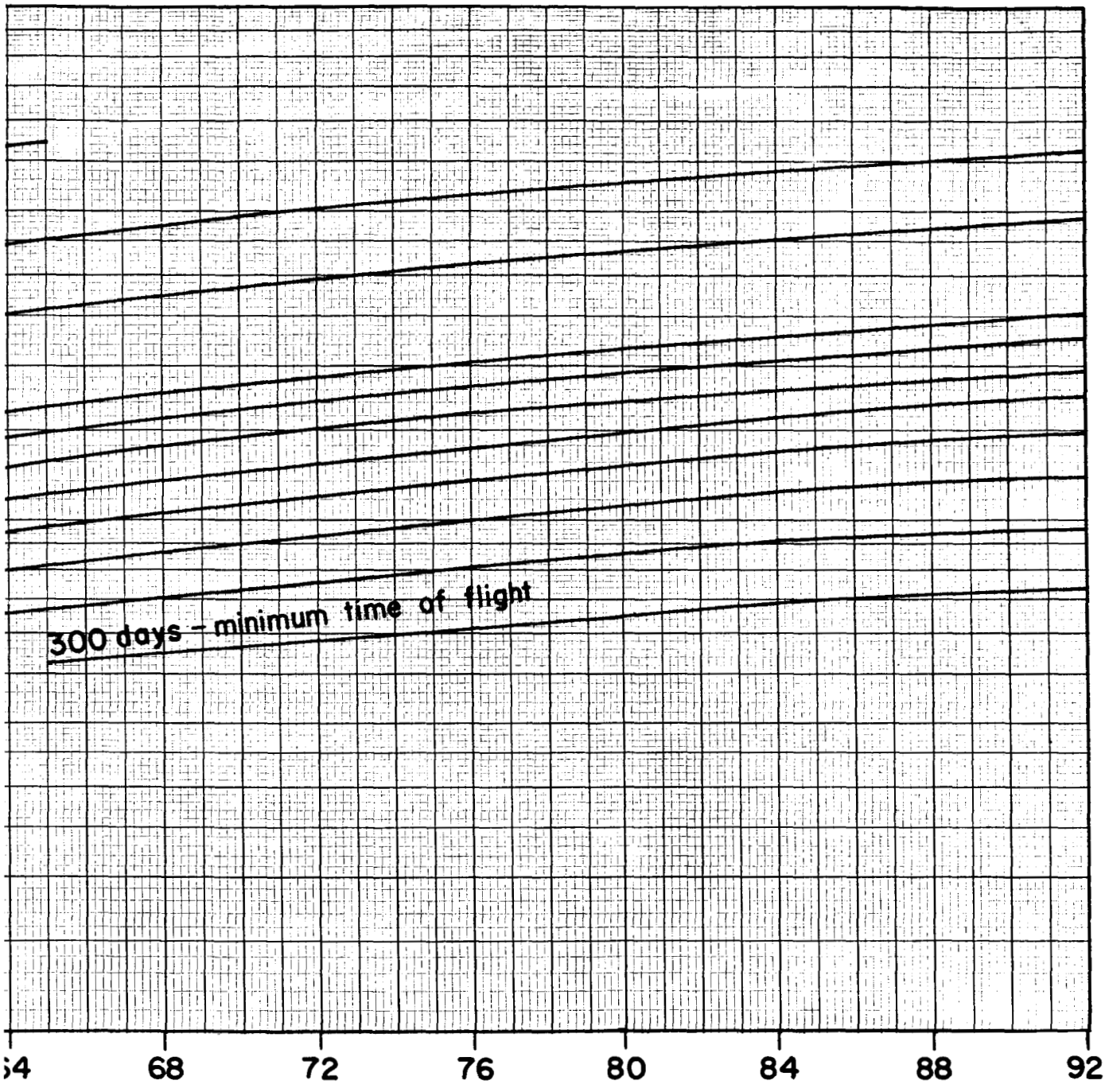

PROBES WITH JUPITER SWINGBY

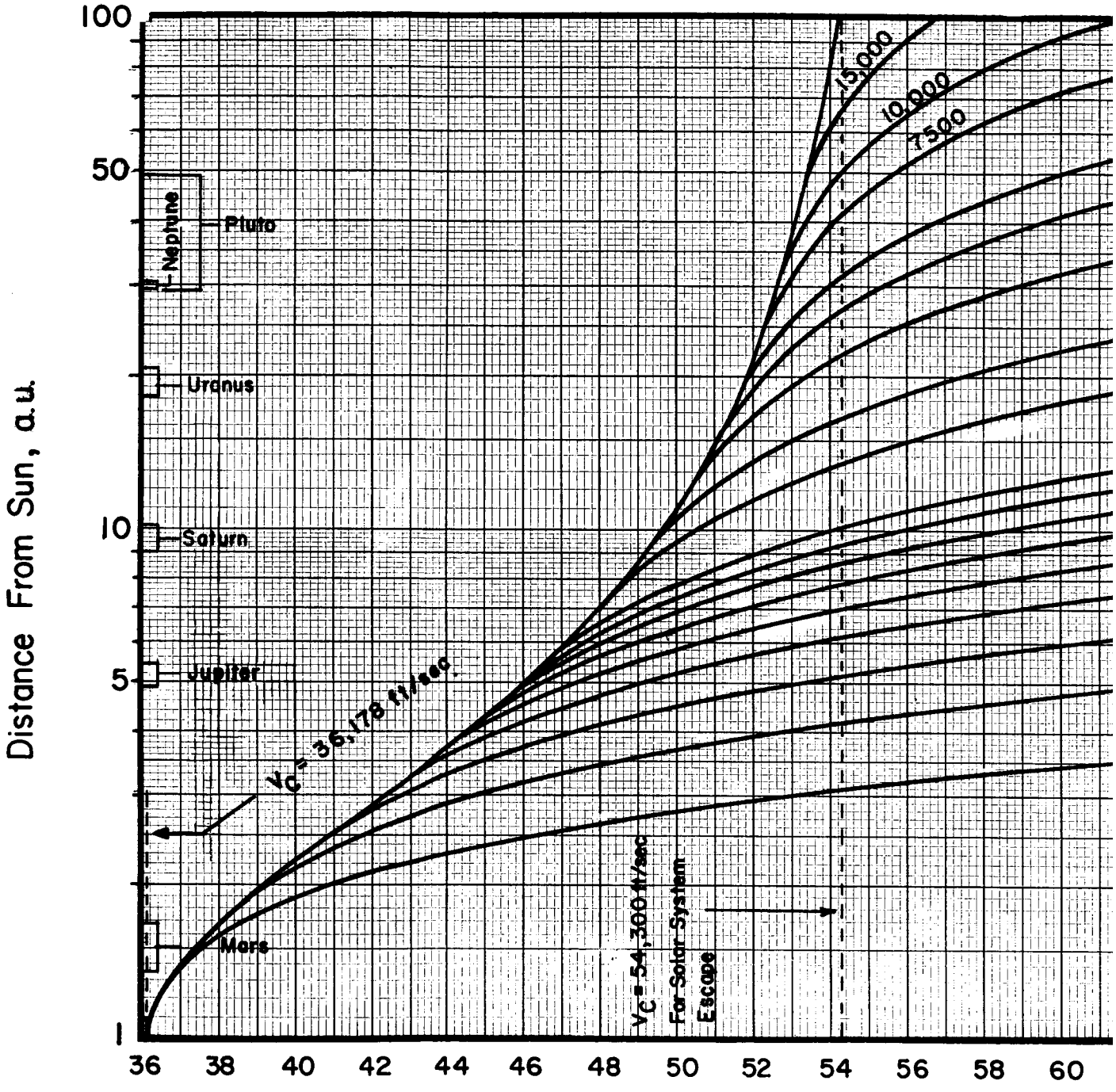

FIGURE 2. VELOCITY REQUIRE
FOR DIRECT FLIGH

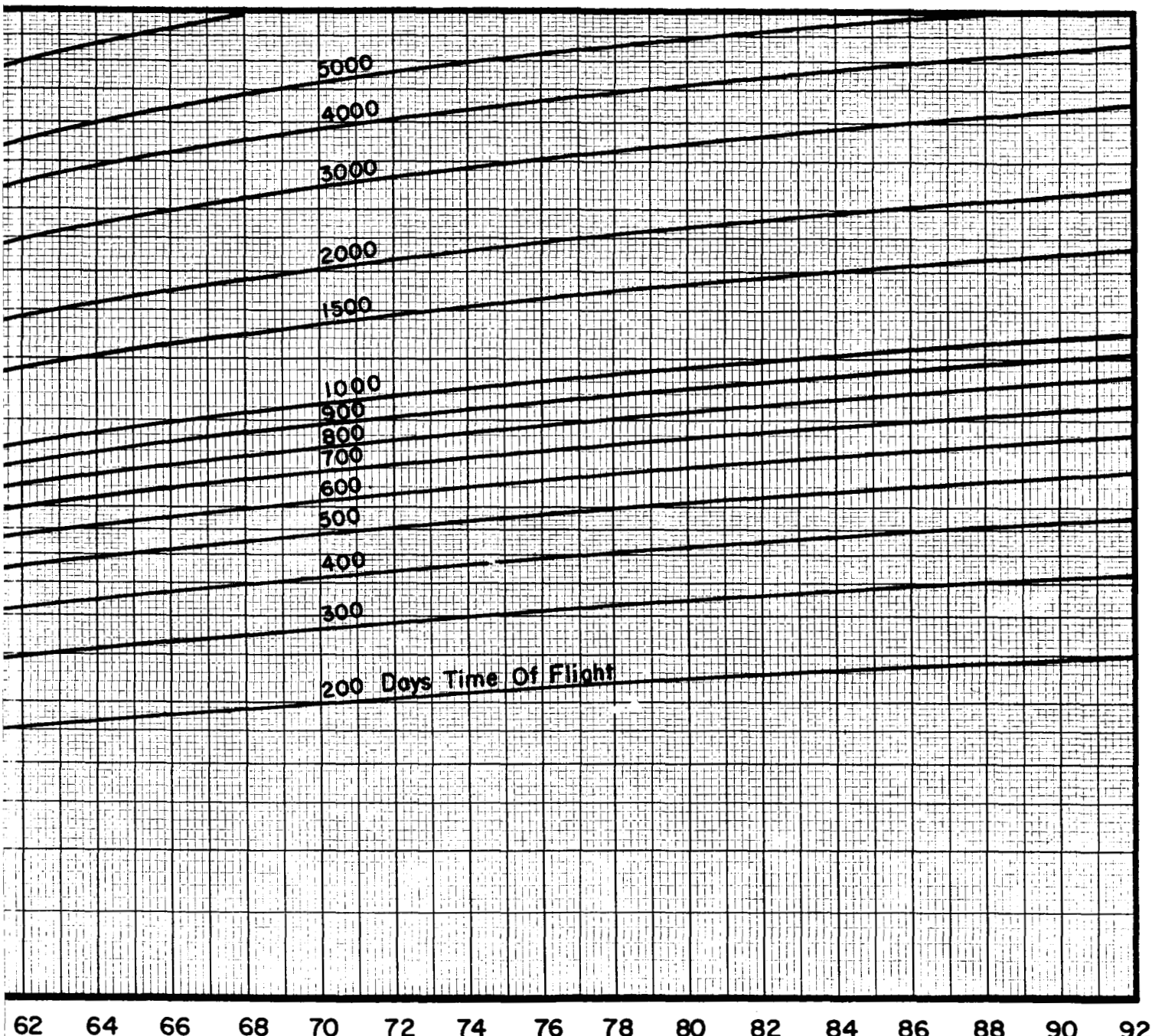

62 64 66 68 70 72 74 76 78 80 82 84 86 88 90 92

ft/sec X 10^{-3}

D FOR OUTER PLANETARY PROBES
T

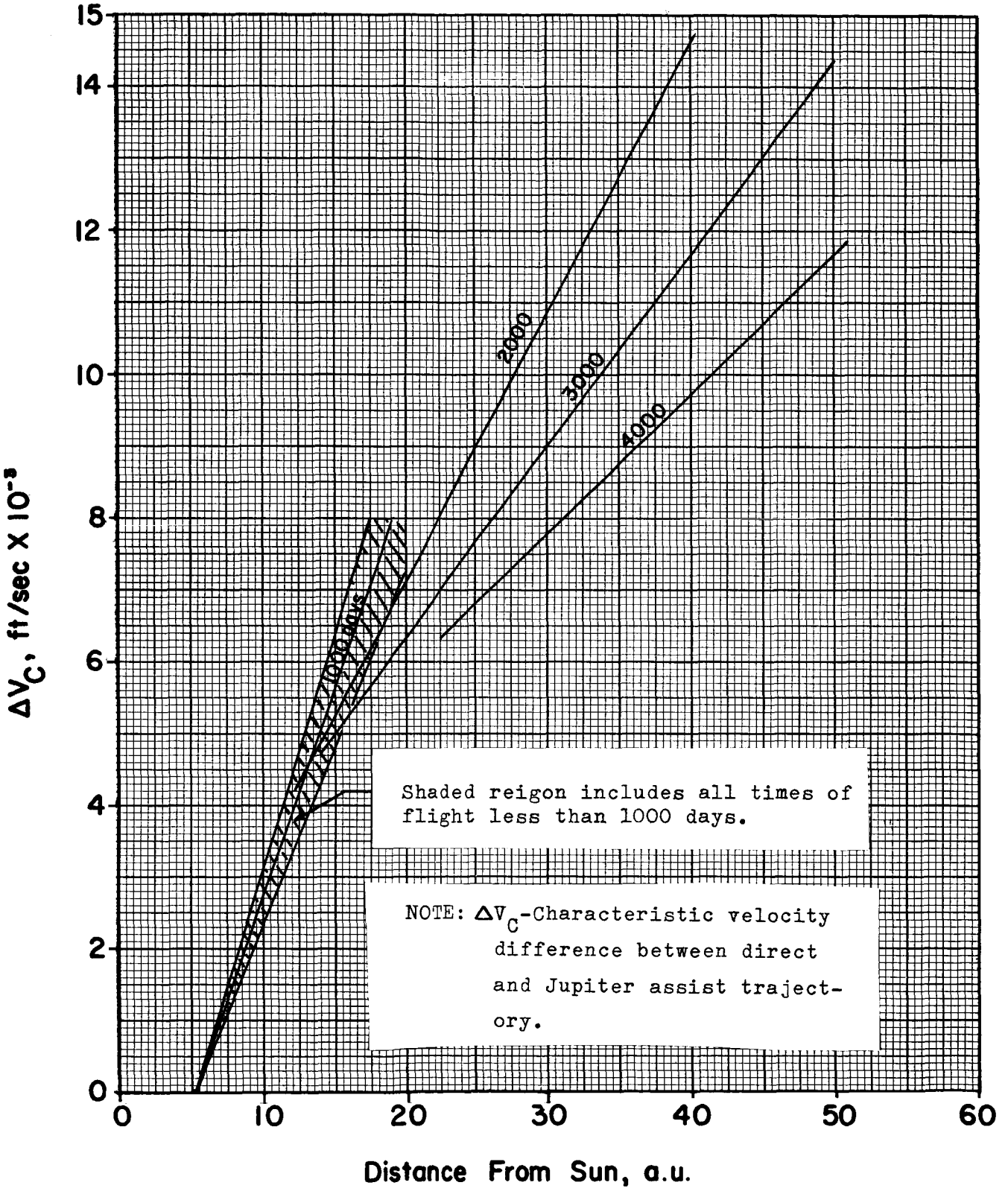

FIGURE 3 . EQUIVALENT VELOCITY FOR JUPITER SWINGBY

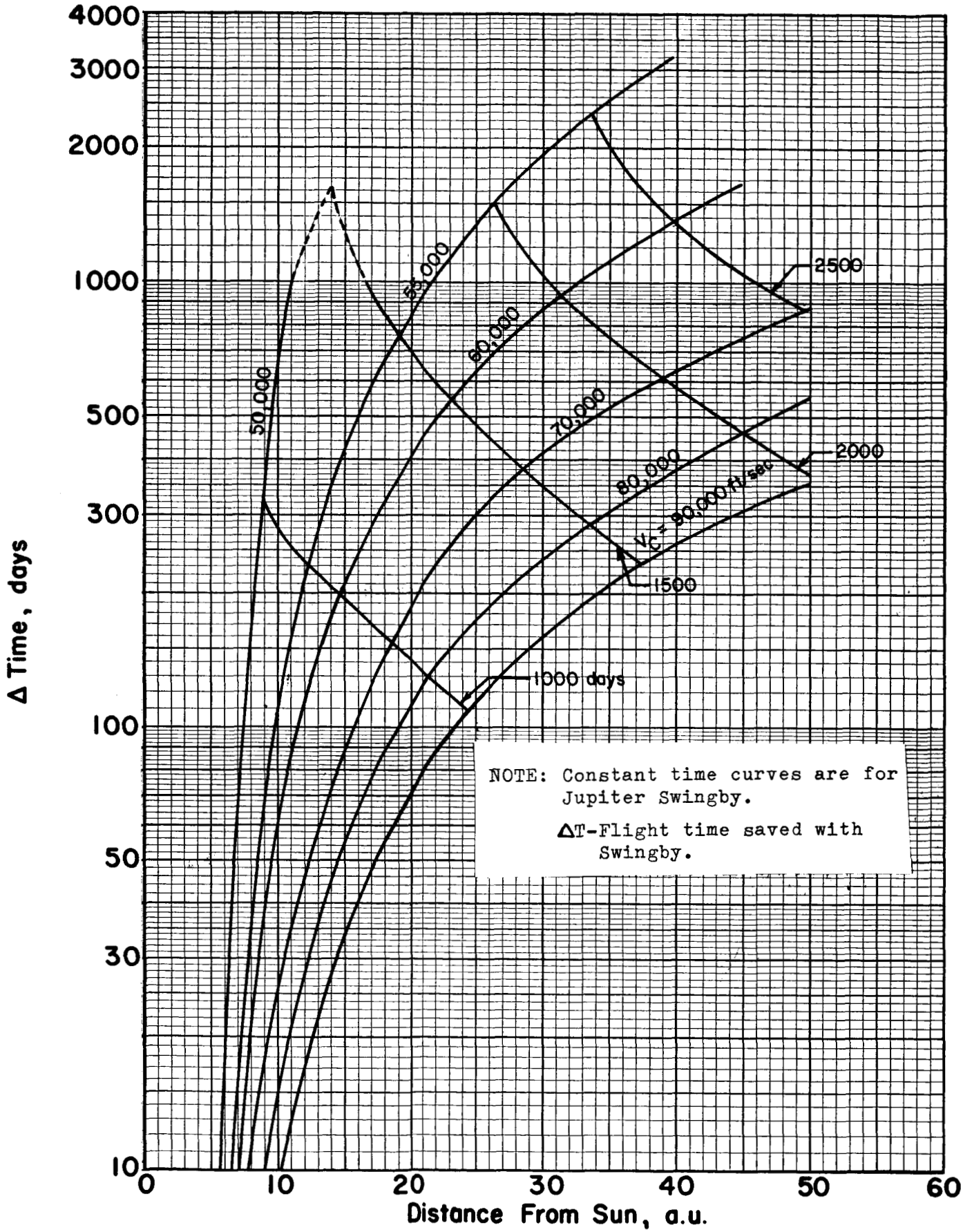

FIGURE 4. FLIGHT TIME REDUCTION FOR JUPITER ASSIST

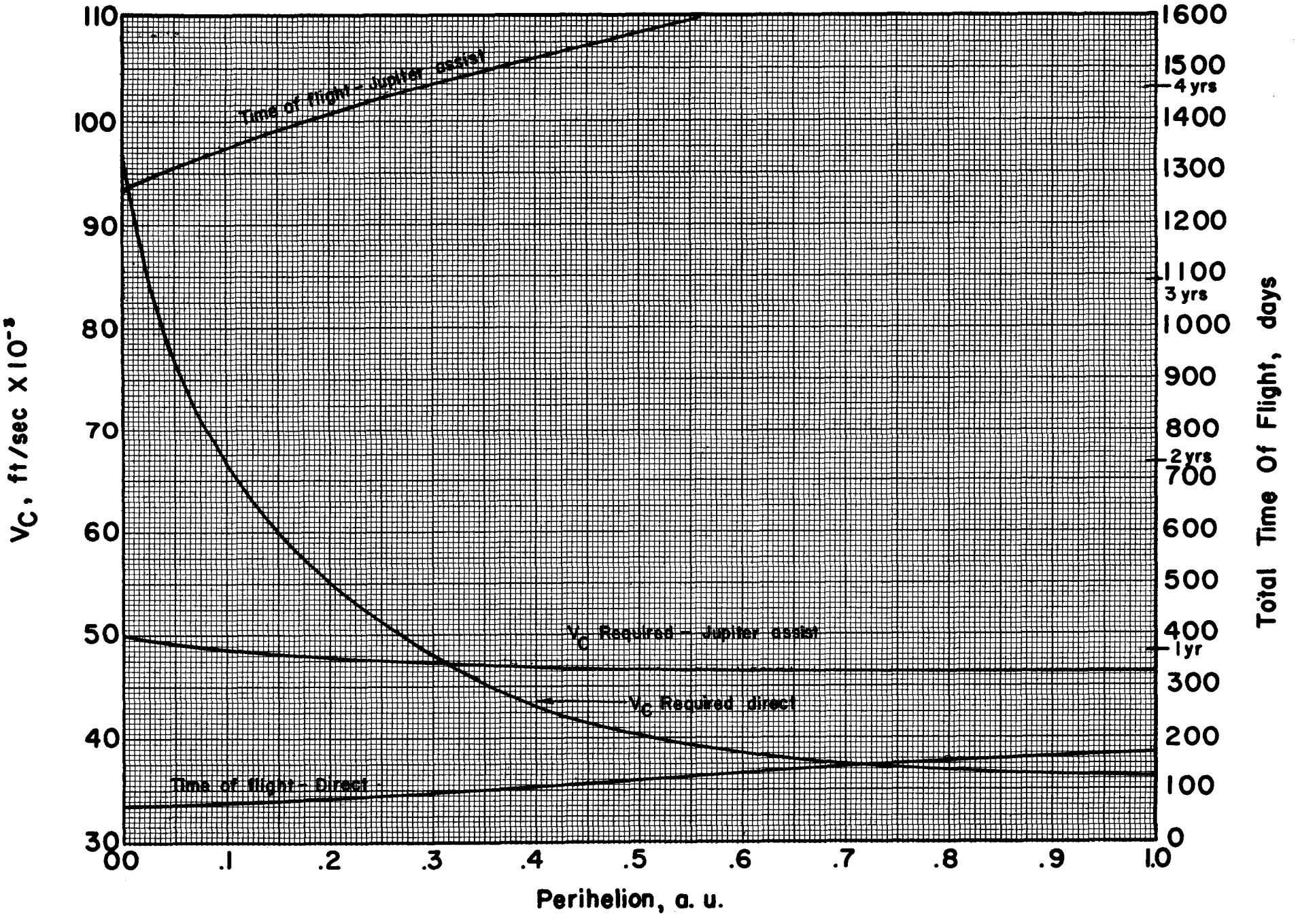

FIGURE 5. SOLAR PROBE COMPARISON

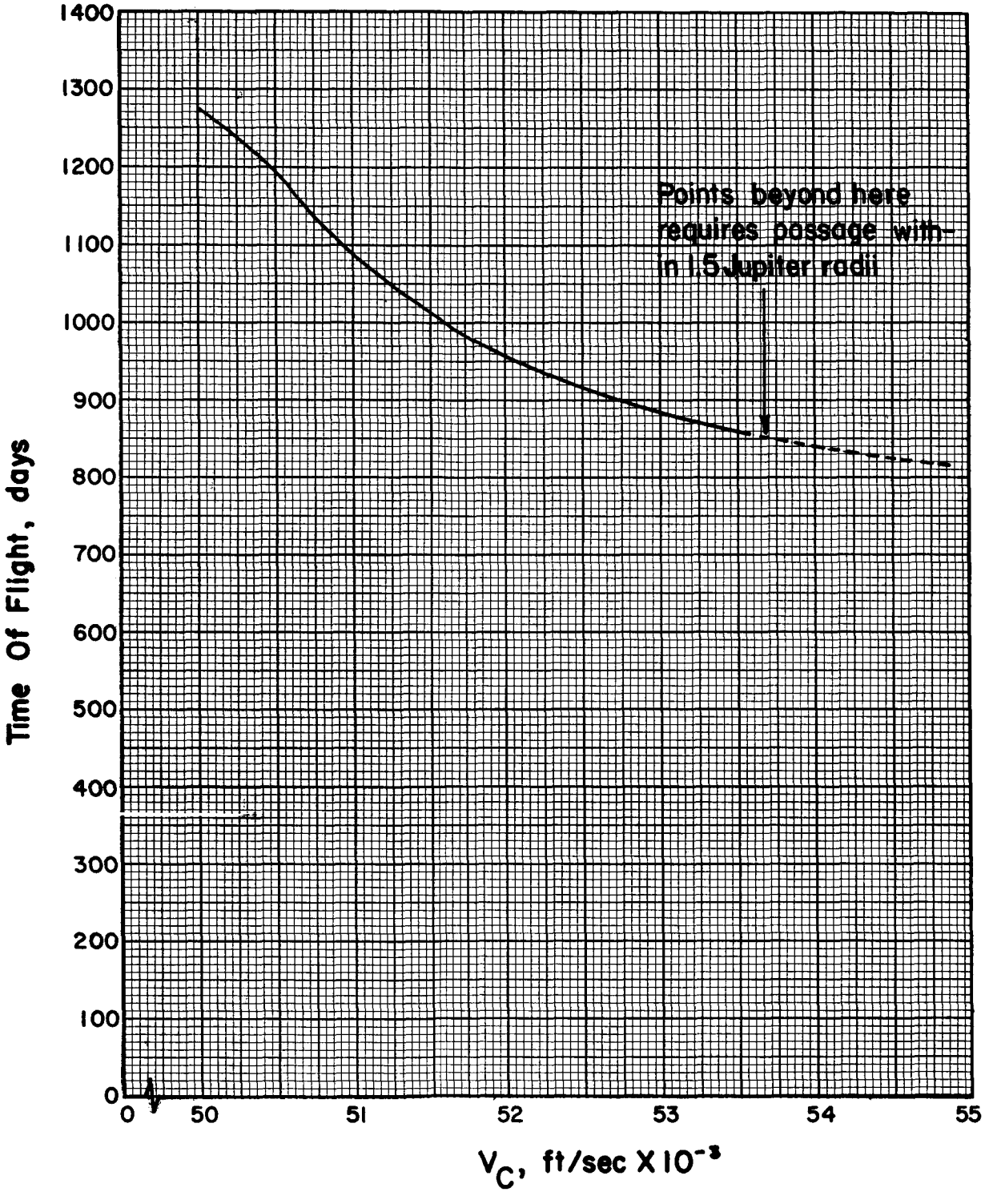

FIGURE 6. VELOCITY- FLIGHT TIME TRADE-OFF FOR SOLAR IMPACT PROBES USING JUPITER ASSIST

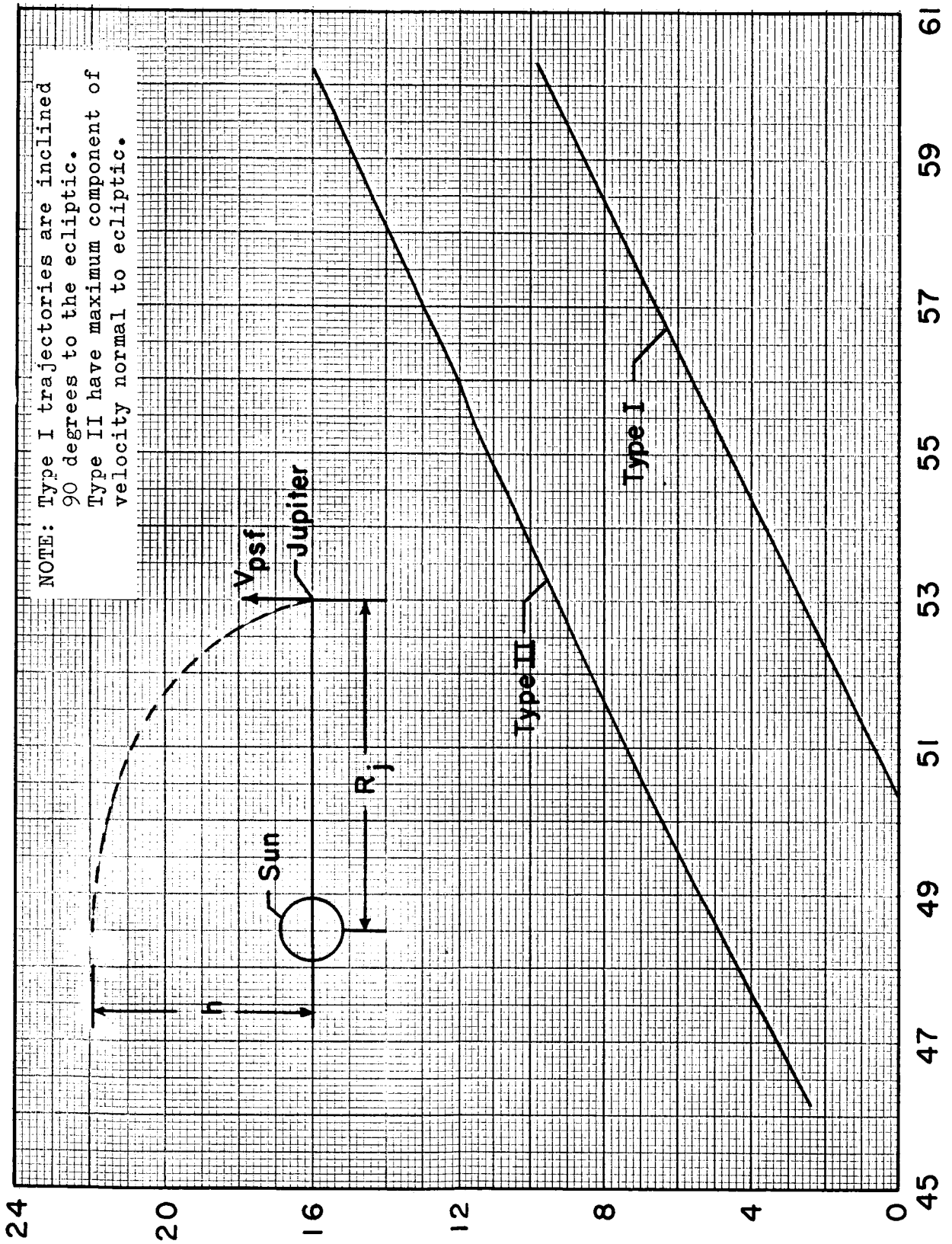

FIGURE 7. DISTANCE FROM ECLIPTIC AT SUN PASSAGE

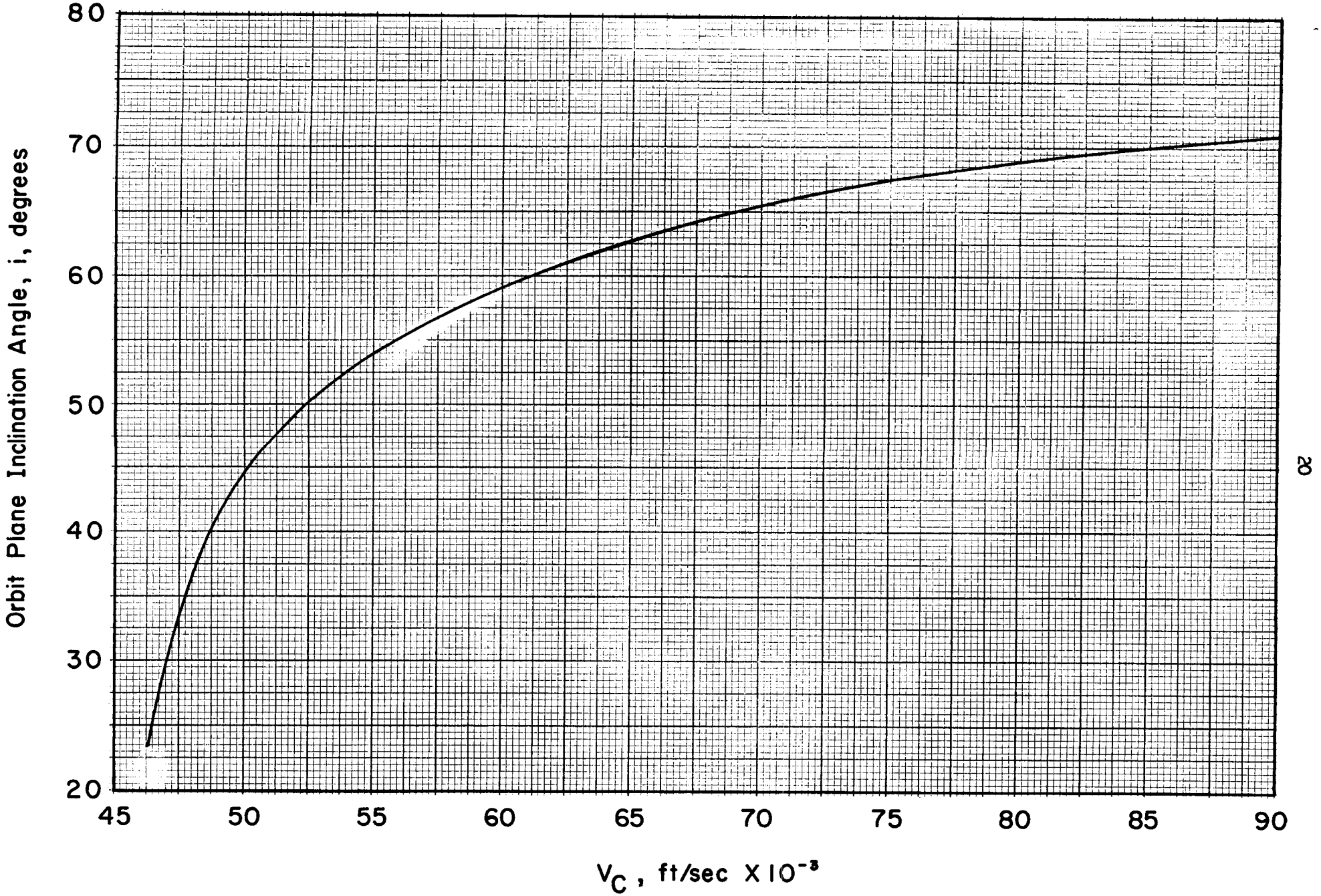

FIGURE 8. INCLINATION ANGLE VERSUS CHARACTERISTIC VELOCITY, TYPE II TRAJECTORIES

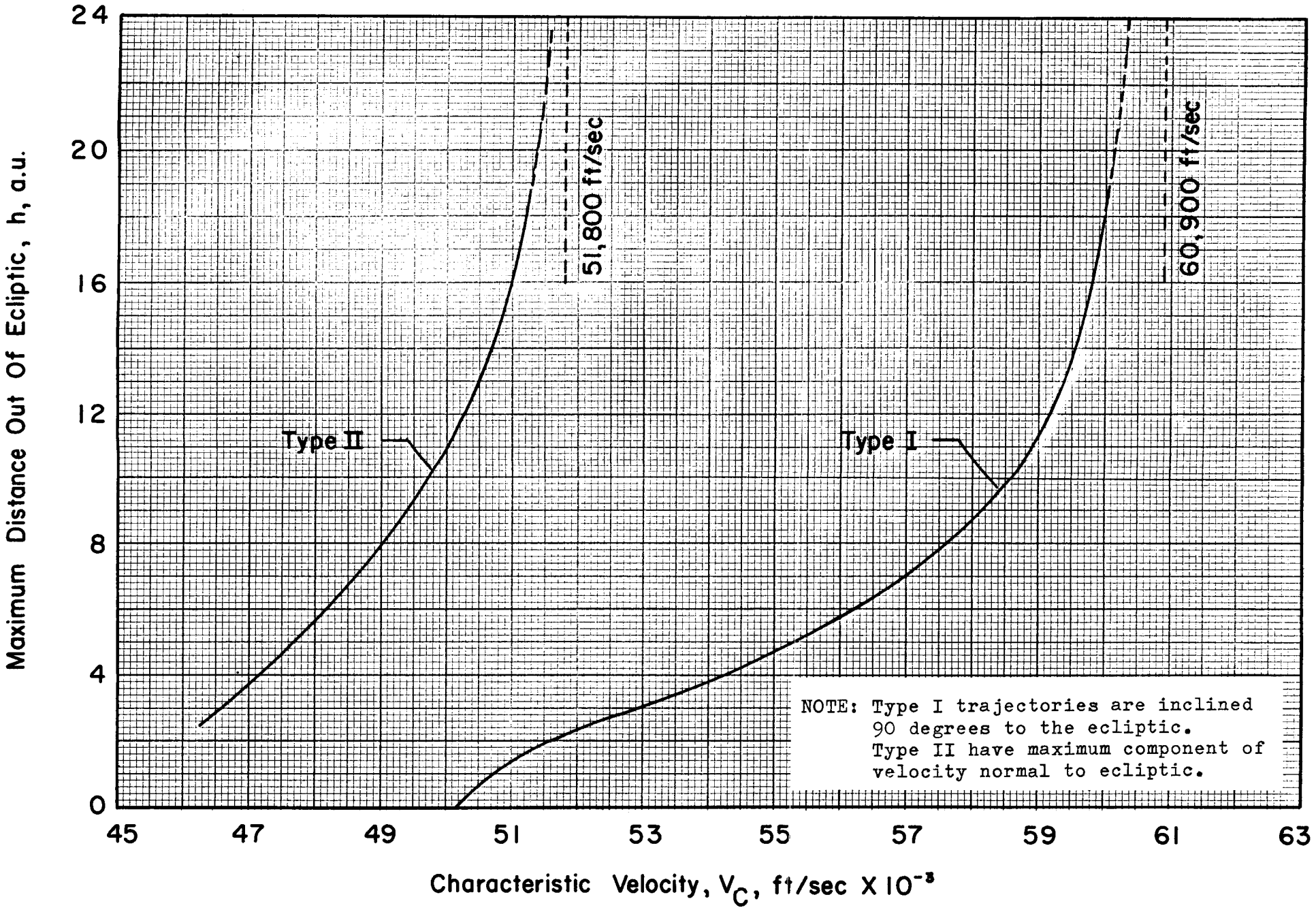

FIGURE 9. DISTANCE OUT OF ECLIPTIC FOR JUPITER SWINGBY

APPENDIX A

REFERENCES

1. M. W. Hunter, II, "Future Unmanned Exploration of the Solar System", Astronautics and Aeronautics, Vol. 2, No. 5, May, 1964, pp 16-26.

2. J. Niehoff, "An Analysis of Gravity-Assisted Trajectories in the Ecliptic Plane", IITRI Report No. T-12, May 25, 1965.

3. R. H. Battin, "The Determination of Round-Trip Planetary Reconnaissance Trajectories", Journal of the Aero/Space Sciences, Vol. 26, No. 9, September, 1959, pp 545-567.

4. G. Knip, Jr., C. L. Zola, "Three Dimensional Sphere-of-Influence Analysis of Interplanetary Trajectories to Mars", NASA TN-D-1199.

5. R. L. Sohn, "Manned Mars Landing and Return Mission", STL Report No. 8572-6011-RU-000, March, 1964.

6. R. L. Sohn, "Venus Swingby for Manned Mars Mission", Journal of Spacecraft, September/October, 1964, pp. 565-567.

7. R. W. Luidens, J. M. Kappraff, "Mars Non-Stop Round-Trip Trajectories", NASA TN-D-2605, January, 1965.

8. J. M. Deerwester, "Initial Mass Savings Associated with the Swingby Mode of Mars Round Trips", AIAA Second Aerospace Sciences Meeting, January 25-27, 1965, Preprint No. 65-89.

9. F. G. Casal, S. Ross, "The Use of Close Venusian Passage During Solar Probe Missions", American Astronautical Society Symposium on Unmanned Exploration of the Solar System, February 8-10, 1965, Preprint No. 65-31.

10. F. M. Sturms, Jr., E. Cutting, "Trajectory Analysis of a 1970 Mission to Mercury via a Close Encounter with Venus", AIAA Second Aerospace Sciences Meeting, January 25-27, 1965, Preprint No. 65-90.

11. M. A. Minovitch, "The Determination and Characteristics of Ballistic Interplanetary Trajectories Under the Influence of Multiple Planetary Attractions", JPL Technical Report No. 32-464.

12. D. F. Lawden, "Perturbation Manoeuvres", Journal of the British Interplanetary Society", Vol. 13, November, 1954, pp 329-334.

13. F. W. Gobetz, "Optimum Transfers Between Hyperbolic Asymptotes", AIAA Journal, Vol. 1, No. 9, September, 1963, pp 2034-2041.

APPENDIX B

NOMENCLATURE FOR APPENDIX B

a_f	Semi-major axis of final heliocentric trajectory
a_i	Semi-major axis of initial heliocentric trajectory
b	Semi-minor axis of final heliocentric trajectory
d	Aiming point miss distance at Jupiter in plane normal to relative velocity vector
e_f	Eccentricity of final heliocentric orbit
e_i	Eccentricity of initial heliocentric orbit
h	Height above the ecliptic plane
i	Inclination angle of final trajectory with respect to ecliptic plane
R	Radial distance from Sun
R_{af}	Radial distance from Sun to aphelion of final heliocentric trajectory
R_E	Radial distance of Earth orbit from Sun
R_h	Radial distance from Sun to final heliocentric trajectory where true anomaly is 90 degrees (Semi-latus rectum)
R_j	Radial distance of Jupiter orbit from Sun
r_j	Radius of Jupiter
R_{pf}	Radial distance from Sun to perihelion of final heliocentric trajectory
r_{pj}	Distance from center of Jupiter to perijove of swingby trajectory
t_{af}	Time of flight from swingby to aphelion of final heliocentric trajectory
t_f	Total time of flight
t_i	Time of flight from Earth launch to encounter
t_{jf}	Time of flight from perihelion to encounter for final heliocentric trajectory
t_{rf}	Time of flight from perihelion to any radial distance for final heliocentric trajectory

V_C	Characteristic velocity at 100 nautical mile reference altitude
V_E	Velocity of Earth in its orbit
V_e	Earth escape velocity at 100 nautical mile reference altitude
VHL	Hyperbolic excess velocity after Earth launch
V_j	Velocity of the planet
V_{pj}	Initial relative velocity of spacecraft with respect to planet
V_{ps}	Velocity of spacecraft with respect to Sun
V_{psf}	Final heliocentric velocity after planetary encounter
V_{psi}	Velocity of spacecraft with respect to Sun at planetary encounter
β_f	Flight path angle, from the radial direction, of the final heliocentric orbit after planetary encounter
β_i	Flight path angle, from the radial direction, of the initial heliocentric orbit at planetary encounter
γ	Turning angle of relative velocity vector at encounter
μ_j	Gravitational constant for Jupiter
μ_s	Gravitational constant for the Sun
ρ	Angle between the initial relative velocity and the planet's velocity vector
θ	True anomaly of heliocentric orbit, measured from perihelion
θ_f	True anomaly of final heliocentric orbit
θ_i	True anomaly of initial heliocentric orbit

COMPUTATIONAL PROCEDURE

The specific equations used in this study were derived in a manner similar to that used for several of the papers listed in the bibliography. In this approach, a patched conic technique was used whereby only one celestial body was assumed to be attracting the spacecraft at any one time. Furthermore, the attracting body was represented as an ideal central force field wherein the gravitational attraction is toward the center and obeys the inverse square law.

A further computational simplification was realized by assuming that both the Earth and planet encountered have a sphere of influence of zero radius in the Sun-centered frame of reference of Figure B-1. A more precise treatment would employ a finite radius about each planet wherein the influence of the planet would dominate that of the Sun. For example, for Jupiter this sphere of influence exceeds a radius of 0.3 a.u., but the effect of neglecting this distance in computing the initial velocity relative to Jupiter is not felt to be significant for our purposes. In addition, the Earth and planet encountered are assumed to be in co-planar circular orbits and all spacecraft trajectories lie in this plane, except for those orbits which are specifically deflected out of the ecliptic plane after Jupiter encounter.

A flow diagram of the trajectory calculations performed on a CDC-3400 computer is shown in Figure B-2. The computational sequence began with the selection of a value of V_C, the characteristic velocity at a reference altitude of 100 nautical miles above the Earth. The hyperbolic excess velocity after Earth escape is given by

$$VHL = \sqrt{V_C^2 - V_e^2} \qquad (1)$$

where V_e is the Earth escape velocity. The perihelion velocity of the initial heliocentric orbit was obtained by adding the velocity of the Earth about the Sun to the hyperbolic excess velocity

$$V_{ps} = VHL + V_E \tag{2}$$

where V_{ps} is the perihelion velocity and V_E is the Earth circular velocity about the Sun.

Establishing the perihelion velocity, V_{ps}, will, in turn, determine the geometry of the initial heliocentric orbit. The eccentricity of the initial orbit is given by the following equation:

$$e_i = \frac{R_E V_{ps}^2}{\mu_s} - 1 \tag{3}$$

where μ_s is the gravitational constant of the Sun and R_E is the Earth's orbital radius. Referring to Figure B-1, it is now possible to determine the spacecraft's location and velocity vector at a particular radial distance from the Sun.

Let R_j denote the orbital radius of the planet to be encountered. Then the spacecraft's location, velocity magnitude and direction (heading angle) were calculated by the following equations:

$$\theta_i = \cos^{-1}\left\{ \frac{R_E}{R_j}\left(\frac{1}{e_i} + 1\right) - \frac{1}{e_i} \right\} \tag{4}$$

$$V_{psi} = \sqrt{V_{ps}^2 - \frac{2\mu_s}{R_E}\left(1 - \frac{R_E}{R_j}\right)} \tag{5}$$

$$\beta_i = \tan^{-1}\left\{ \frac{1 + e_i \cos\theta_i}{e_i \sin\theta_i} \right\} \tag{6}$$

It should be noted that the selection of V_C completely defines the initial conditions at the planet to be encountered, within the assumptions of this analysis.

The final calculation which was made with reference to the initial orbit was the flight time from perihelion to encounter. The time of flight calculation is given by one of two expressions, depending on the type of orbit. For e_i greater than zero and less than one (elliptical orbits), the flight time is given by

$$t_i = \frac{a_i^{3/2}}{\sqrt{\mu_s}} \left\{ 2\tan^{-1}\left(\sqrt{\frac{1-e_i}{1+e_i}} \tan\frac{1}{2}\theta_i \right) - \frac{e_i\sqrt{1-e_i^2}\,\sin\theta_i}{1+e_i\cos\theta_i} \right\} \tag{7}$$

where

$$a_i = \frac{R_E}{2 - \frac{R_E V_{ps}^2}{\mu_s}} \tag{8}$$

and

$$\theta_i = \cos^{-1}\left\{ \frac{R_E}{R_j}\left(\frac{1}{e_i}+1\right) - \frac{1}{e_i} \right\} \tag{9}$$

For e_i greater than one (hyperbolic orbit), the flight time expression becomes

$$t_i = \frac{a_i^{3/2}}{\sqrt{\mu_s}} \left\{ \frac{e_i\sqrt{e_i^2-1}\,\sin\theta_i}{1+e_i\cos\theta_i} - \ln\left(\frac{\sqrt{e_i+1} + \sqrt{e_i-1}\,\tan\frac{1}{2}\theta_i}{\sqrt{e_i+1} - \sqrt{e_i-1}\,\tan\frac{1}{2}\theta_i} \right) \right\} \tag{10}$$

where

$$a_i = \frac{R_E}{\frac{R_E V_{psi}^2}{\mu_s} - 2} \tag{11}$$

and θ_i is the same as above.

At this point, the parameters associated with the encounter were determined. The effect of a swingby is to turn the initial relative velocity vector through some angle γ, see Figure B-3. The initial relative velocity is given in terms of the initial conditions at encounter by the following expressions:

$$\rho = \tan^{-1}\left\{ \frac{V_{psi}\cos\beta_i}{V_j - V_{psi}\sin\beta_i} \right\} \tag{12}$$

and

$$V_{pj} = \frac{V_{psi} \cos \beta_i}{\sin \rho} \tag{13}$$

where V_j is the velocity of the planet, ρ is the angle between the initial relative velocity and the planet's velocity, and V_{pj} is the initial relative velocity (see Figure B-3).

The calculation procedure was to select a given turning angle, γ, within the possible range, and then to determine the new heliocentric orbit. For each value of γ, the relative velocity vector assumes a new orientation with respect to the velocity vector of the planet encountered, as seen in Figure B-3. To determine the possible turning angle, γ can be expressed as

$$\gamma = \pm 2 \cot^{-1} \left\{ \left(\frac{r_{pj}}{r_j} \right)^2 \left(\frac{r_j V_{pj}^2}{\mu_j} \right)^2 + 2 \left(\frac{r_{pj}}{r_j} \right) \left(\frac{r_j V_{pj}^2}{\mu_i} \right) \right\}^{1/2} \tag{14}$$

where r_{pj} is the perijove distance, r_j is the planet's radius, and μ_j is the planet's gravitational constant (see Figures B-4 and B-5). The only real limitation on turning angle is seen to be the necessity to avoid impact with the surface $\left(\frac{r_{pj}}{r_j} = 1 \right)$. This places a constraint on the maximum turning angle which varies with V_c. In practice, it would also be necessary to avoid the planet's atmosphere. For this reason, no turning angles requiring passage closer than $\frac{r_{pj}}{r_j} = 1.5$ were considered in the computations. Therefore, the range of γ is given by

$$\gamma = \pm 2 \cot^{-1} \left\{ 2.25 \left(\frac{r_j V_{pj}^2}{\mu_j} \right)^2 + 3 \left(\frac{r_j V_{pj}^2}{\mu_j} \right) \right\}^{1/2} \tag{15}$$

The selection of γ also determines a miss distance, d, which is useful for guidance. The miss distance is given by the expression

$$d = \frac{\mu_j}{V_{pj}^2} \cot \frac{\gamma}{2} \tag{16}$$

Figures B-4 and B-5 are plots of turning angle versus miss distance for various V_C. These Figures are for the planets Jupiter and Mars.

Referring to Figure B-3, the new heliocentric velocity of the spacecraft increases if γ is in the counter-clockwise direction (positive γ), corresponding to passage behind the planet. This is the case depicted in Figure B-3. If passage is ahead of the planet, γ will be in a clockwise direction (negative γ), and the heliocentric velocity will be reduced, in general.

The final heading angle, heliocentric velocity, and eccentricity after encounter are given by

$$\beta_f = \tan^{-1} \left\{ \frac{V_j - V_{pj} \cos(\rho + \gamma)}{V_{pj} \sin(\rho + \gamma)} \right\} \tag{17}$$

$$V_{psf} = \frac{V_{pj} \sin(\rho + \gamma)}{\cos \beta_f} \tag{18}$$

and

$$e_f = \left\{ 1 - \frac{V_{psf}^2 R_j \sin^2 \beta_f}{\mu_s} \left(2 - \frac{V_{psf}^2 R_j}{\mu_s} \right) \right\}^{1/2} \tag{19}$$

Each new heliocentric orbit, corresponding to each selected value of γ, was tested to determine if it were elliptical or hyperbolic. If elliptical $(0 < e_f < 1)$, the aphelion distance and the total time from Earth launch to aphelion were computed. If the new orbit were hyperbolic $(e_f > 1)$, the times of flight to various specified radial distances from the Sun were computed.

If e_f is between zero and one, the aphelion distance is given by

$$R_{af} = a_f\ (1+e_f) \tag{20}$$

where

$$a_f = \frac{R_j}{2 - \frac{R_j\ V_{psf}^2}{\mu_s}} \tag{21}$$

The time of flight from encounter to aphelion was calculated by first calculating the time of flight from perihelion to aphelion and then subtracting the time from perihelion to encounter. The final expression for the time of flight from encounter to aphelion was

$$t_{af} = \frac{a_f^{3/2}}{\sqrt{\mu_s}} \left\{ \pi - \left[2\tan^{-1}\left(\sqrt{\frac{1-e_f}{1+e_f}}\ \tan\tfrac{1}{2}\theta_f - \frac{e_f\sqrt{1-e_f^2}\sin\theta_f}{1+e_f\cos\theta_f} \right) \right] \right\} \tag{22}$$

where

$$\theta_f = \cos^{-1}\left\{ \frac{1}{e_f}\left[\frac{a_f(1-e_f^2)}{R_j} - 1 \right] \right\} \tag{23}$$

The total time of flight was then obtained by adding the flight time from launch to encounter, t_i, to t_{af}:

$$t_f = t_{af} + t_i \tag{24}$$

If $e_f > 1$ (hyperbolic orbit), a range of radial distance was specified and the times of flight to these distances were calculated. The time of flight from perihelion to R, some radial distance, is given by

$$t_{rf} = \frac{a_f^{3/2}}{\sqrt{\mu_s}} \left\{ \frac{e_f\sqrt{e_f^2-1}\sin\theta}{1+e_f\cos\theta} - \ln\left(\frac{\sqrt{e_f+1} + \sqrt{e_f-1}\ \tan\frac{1}{2}\theta}{\sqrt{e_f+1} - \sqrt{e_f-1}\tan\frac{1}{2}\theta} \right) \right\} \tag{25}$$

where

$$a_f = \frac{R_j}{\frac{R_j\ V_{psf}^2}{\mu_s} - 2} \tag{26}$$

and

$$\theta = \cos^{-1}\left\{ \frac{1}{e_f}\left[(1+e_f)\frac{R_{pf}}{R} - 1 \right] \right\} \tag{27}$$

The perihelion distance, R_{pf}, in Equation 27 for θ was calculated from

$$R_{pf} = \frac{R_j (1 + e_f \cos \theta_f)}{1 + e_f} \tag{28}$$

where

$$\theta_f = \cos^{-1}\left\{ \frac{1}{e_f} \left[\frac{a_f(e_f^2 - 1)}{R_j} - 1 \right] \right\} \tag{29}$$

The flight time from perihelion to encounter must be subtracted from t_{rf} and this result added to t_i to obtain the total flight time.

With t_{jf} denoting flight time from perihelion to encounter,

$$t_{jf} = \frac{a_f^{3/2}}{\sqrt{\mu_s}} \left\{ \frac{e_f \sqrt{e_f^2 - 1} \sin \theta_f}{1 + e_f \cos \theta_f} - \ln \left(\frac{\sqrt{e_f + 1} + \sqrt{e_f - 1} \tan \frac{1}{2} \theta_f}{\sqrt{e_f + 1} - \sqrt{e_f - 1} \tan \frac{1}{2} \theta_f} \right) \right\} \tag{30}$$

and the total flight time is

$$t_f = t_i + t_{rf} - t_{jf} \tag{31}$$

After the range of γ's was completed, a new value of V_C was selected and the complete process just described was repeated.

To minimize the flight time for a value of V_C and specified radii, the turning angle yielding minimum time was determined from an examination of the computer print-out. The associated minimum time of flight was plotted versus radial distance for each selected V_C. Finally, a cross plot was made for fixed time of flight to illustrate the relationship between radial distance and V_C. These plots appear in the body of the text.

For solar probes, the perihelion of the new heliocentric trajectory was minimized by turning the relative velocity vector so that the new heliocentric velocity is made as small as possible. Figure B-3 shows that this is accomplished by turning the relative velocity vector clockwise (passage ahead of the planet) such that the final relative velocity is opposite to the direction of the planet's velocity vector. The perihelion can be reduced to zero if the relative velocity vector is equal in magnitude

to the velocity of the planet encountered and if the turning angle can be negotiated. For example, a Jupiter swingby can be used to reduce the perihelion to zero if V_C is approximately equal to 50,400 ft/sec.

A particular type of trajectory occurs for those solar probes which impact on the Sun after Jupiter encounter. At Jupiter, the relative velocity vector is turned clockwise (passage ahead of Jupiter) in such a way that the final heliocentric velocity is directed radially inward toward the Sun. For this special type of trajectory, from the vis-viva integral,

$$V = \frac{dR}{dt} = -\sqrt{\frac{2\mu_s}{R} - \frac{\mu_s}{a_f}} \tag{32}$$

Inverting Equation 32 and rearranging

$$\Delta t = \sqrt{\frac{a_f}{\mu_s}} \int_R^{R_o} \frac{\sqrt{R}}{\sqrt{2a_f - R}}\, dR \tag{33}$$

Equation 33 is integrated to yield:

$$\Delta t = \sqrt{\frac{a_f}{\mu_s}} \left\{ \sqrt{R(2a_f - R)} - \sqrt{R_o(2a_f - R_o)} \right\} + 2\sqrt{\frac{a_f^3}{\mu_s}} \left\{ \sin^{-1}\sqrt{\frac{2a_f - R}{2a_f}} - \sin^{-1}\sqrt{\frac{2a_f - R_o}{2a_f}} \right\} \tag{34}$$

For the special case, $R_o = R_j$ and R=0, so the time of flight expression is arrived at for the inbound portion of the solar impact probe trajectory:

$$\Delta t = -\sqrt{\frac{a_f}{\mu_s}}\sqrt{R_j(2a_f - R_j)} + 2\sqrt{\frac{a_f^3}{\mu_s}} \left[\frac{\pi}{2} - \sin^{-1}\sqrt{\frac{2a_f - R_j}{2a_f}} \right] \tag{35}$$

The semi-major axis of the perturbed trajectory, a_f, is evaluated from the vis-viva, Equation 32.

OUT-OF-THE-ECLIPTIC ANALYSIS

An orbit out of the ecliptic plane can be accomplished if the probe is disturbed very slightly out of the ecliptic by a mid-course correction and made to pass the encountered planet above or below the ecliptic plane. Then, under the gravitational influence of the planet, the probe will swing into an orbit whose plane is other than the ecliptic. In this section, the interest is in determining the maximum distances that can be obtained from the ecliptic plane using a Jupiter swingby. There will be a maximum distance for each launch velocity, V_C.

Referring to Figure B-3, the initial relative velocity vector was restricted to turning angles for which the locus of possible end points of the final heliocentric velocity vector lie in the ecliptic plane. For the more general case of orbits out of the ecliptic, the locus of possible end points of the final heliocentric velocity vector will lie on a sphere. The excluded region will now become a cone section of some solid angle which is a function of the characteristic launch velocity. The vertex angle of the cone section can be calculated using Figure B-4. Figure B-4 can be used to obtain the possible turning angle, γ , for a given V_C and d/r_j. The vertex angle is then given by

$$\text{vertex angle} = 360^\circ - 2\gamma \ .$$

The selection of two possible swingby trajectories, shown in Figures B-6 and B-7, are considered in detail. Figure B-6 illustrates a trajectory which is inclined 90° to the ecliptic. These trajectories will be denoted as Type I. Figure B-7 represents trajectories which have a maximum final heliocentric velocity component normal to the ecliptic plane, and they will be designated Type II trajectories.

The turning angle required for Type I and II trajectories is equal to or less than 90°. Therefore, if passage distance, $(\frac{r_p}{r_j})$, is limited to 1.5 planet radii, the maximum characteristic earth launch velocity is approximately equal to 60,000 ft/sec.

Referring to Figures B-6 and B-7, the final heliocentric velocity magnitude is given by

$$V_{psf} = \sqrt{V_{pj}^2 \pm V_j^2} \tag{36}$$

where V_{pj} is the relative velocity and V_j is Jupiter's velocity. The plus sign in Equation 1 is used for Type II trajectories and the minus sign for Type I.

Since the aphelion or perihelion of the final orbit is located at encounter, the eccentricity of the new orbit becomes

$$e_f = \frac{V_{psf}^2 R_j}{\mu_s} - 1 \tag{37}$$

To determine the maximum distance from the ecliptic, the expression for the semi-minor axis will be needed. The semi-minor axis is given by

$$b = R_j \sqrt{\frac{1 + e_f}{1 - e_f}} \tag{38}$$

Rewriting Equation 38 in terms of the final heliocentric velocity,

$$b = R_j \sqrt{\frac{(V_{psf}/V_j)^2}{2-(V_{psf}/V_j)^2}} \tag{39}$$

where V_j^2 has been substituted for μ_s/R_j.

The maximum distance out of the ecliptic plane can now be calculated from

$$h = b \sin i, \tag{40}$$

where i is defined as the trajectory's inclination angle. A plot of h versus characteristic velocity for Type I and II trajectories is plotted in Figure 9.

For Type I trajectories, the inclination angle is 90°; therefore from Equation 40 it is apparent that the maximum distance is equal to the semi-minor axis of the trajectory.

The inclination angle for Type II trajectories is given by

$$i = \tan^{-1}\left(\frac{V_{pj}}{V_j}\right) \tag{41}$$

Figure 8 is a plot of inclination angle versus characteristic velocity, V_C.

The distance from the ecliptic plane as the probe passes the Sun is of interest and can be determined for the two types of swingby trajectories analyzed in this section. The distance from the Sun to the probe, at Sun passage is given by

$$R_h = R_j\,(1 + e_f) \tag{42}$$

Substituting for e_f in Equation 42 from Equation 37, R_h is obtained in terms of (V_{psf}/V_j),

$$R_h = R_j\,(V_{psf}/V_j)^2. \tag{43}$$

The distance from the ecliptic plane is obtained by multiplying R_h by sin i:

$$h = R_h \sin i. \tag{44}$$

Figure 7 is a plot of h versus characteristic velocity for both types of orbits.

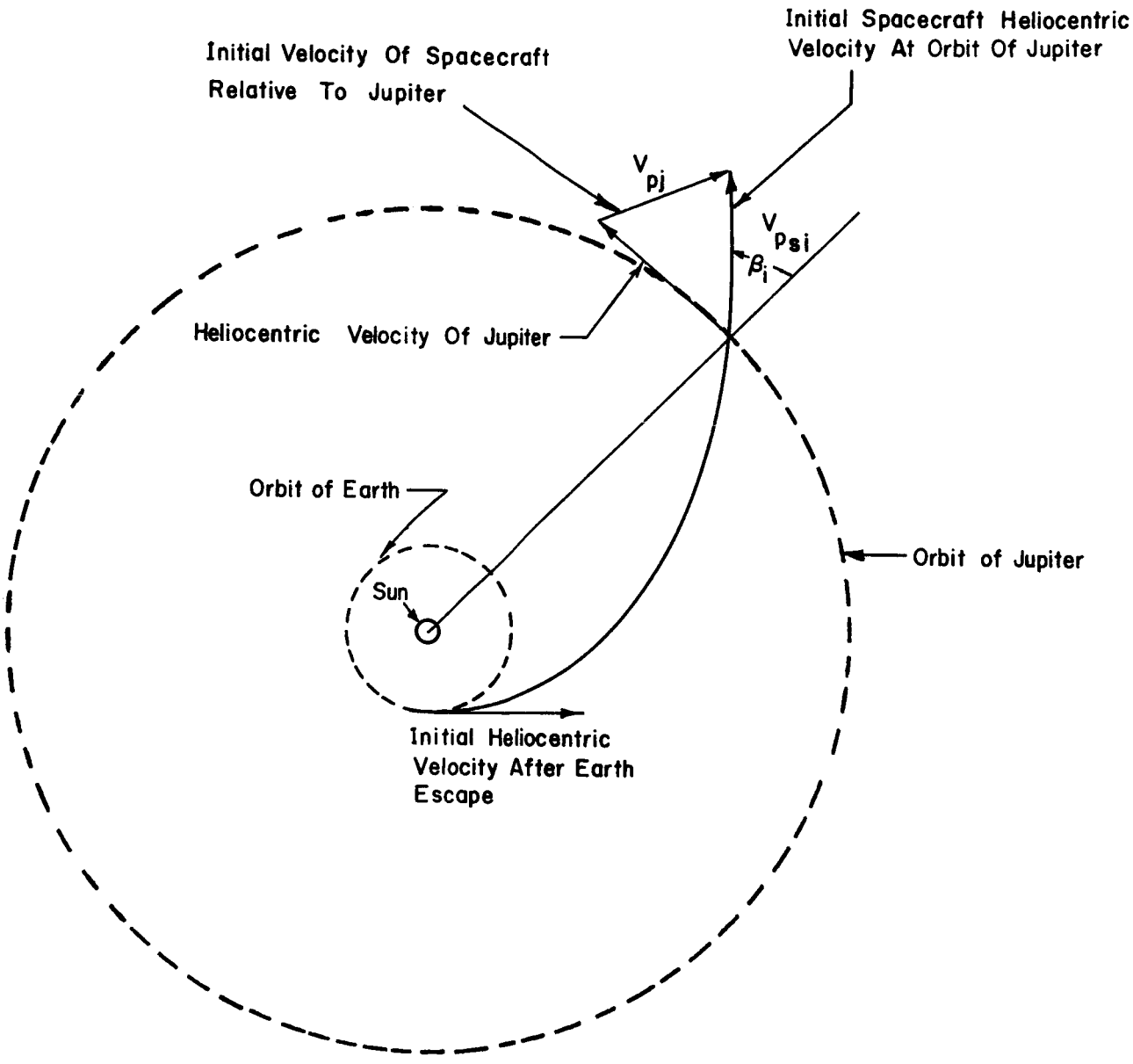

FIGURE B-1. THE INITIAL HELIOCENTRIC ORBIT

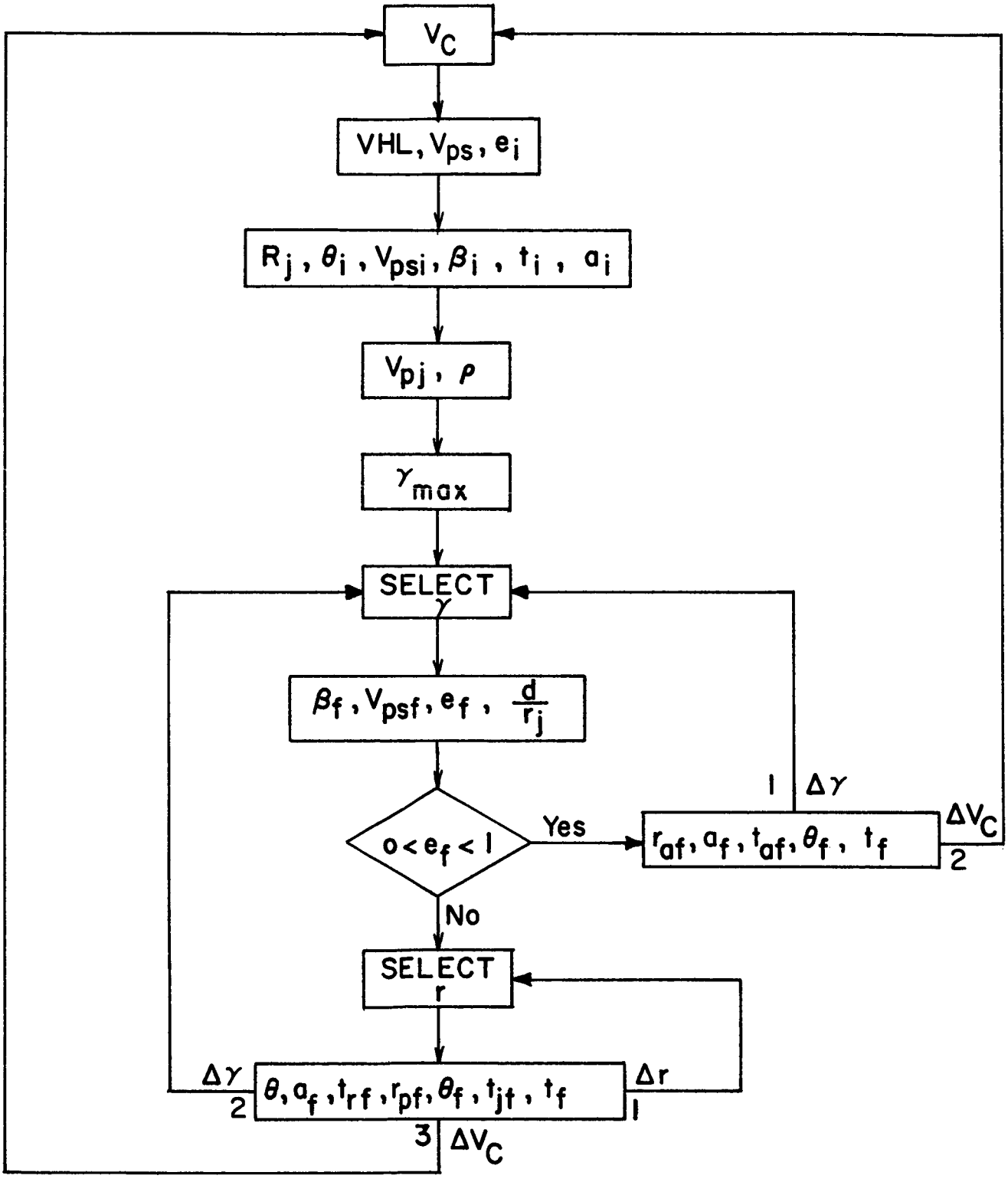

FIGURE B-2. FLOW DIAGRAM FOR TRAJECTORY CALCULATION

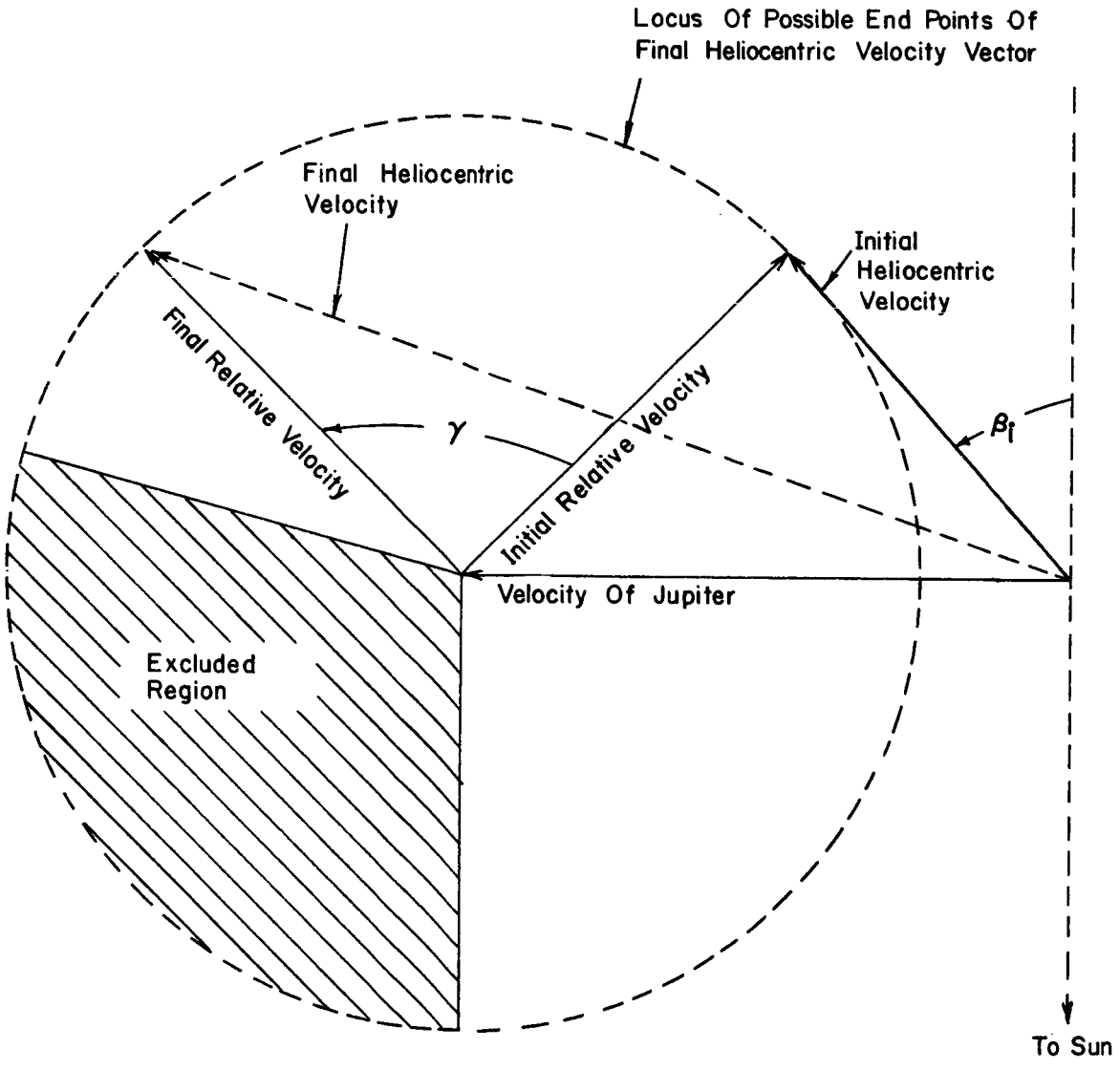

FIGURE B-3. VECTOR DIAGRAM OF ENCOUNTER

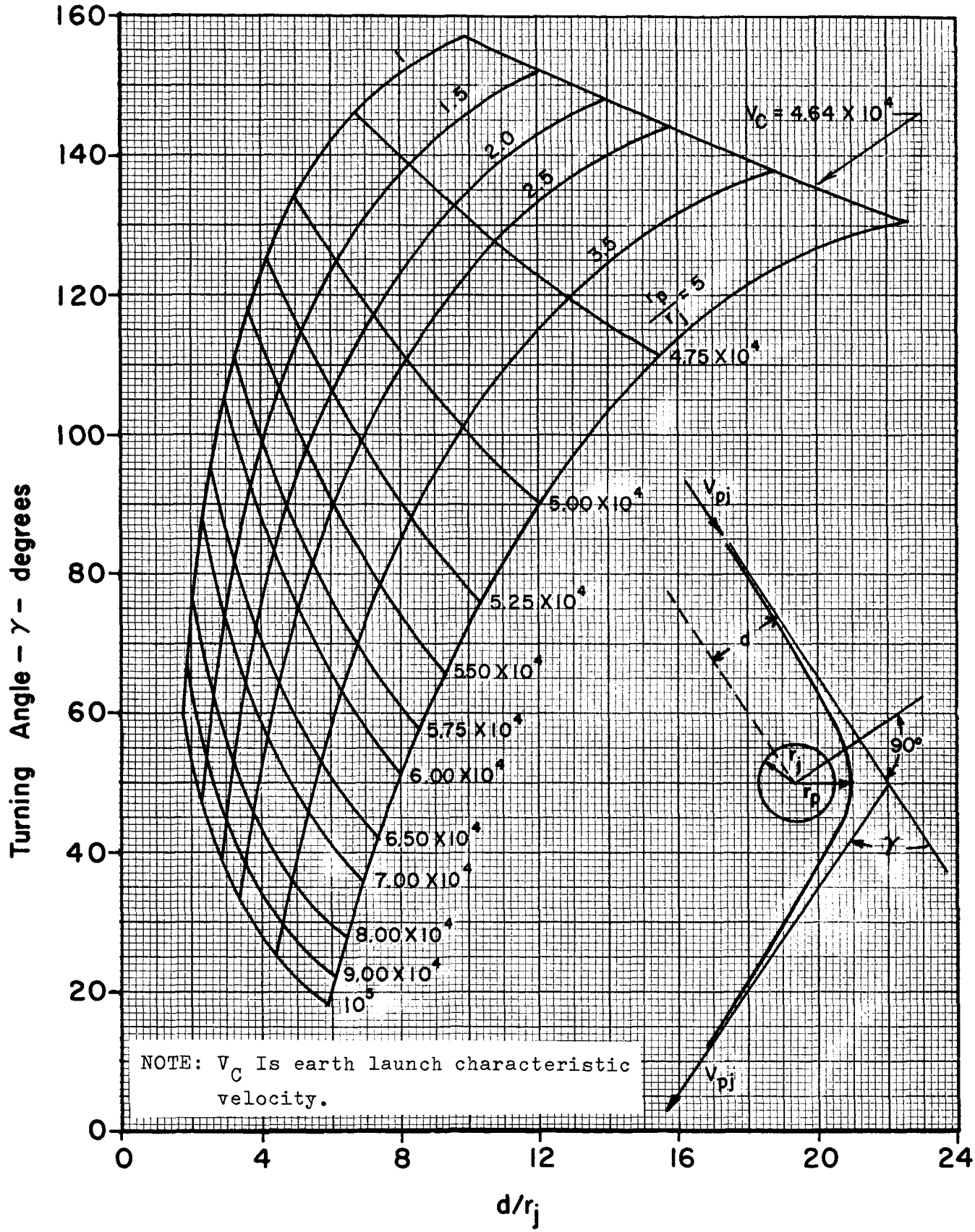

FIGURE B-4. TURNING ANGLE VERSUS MISS DISTANCE AT JUPITER

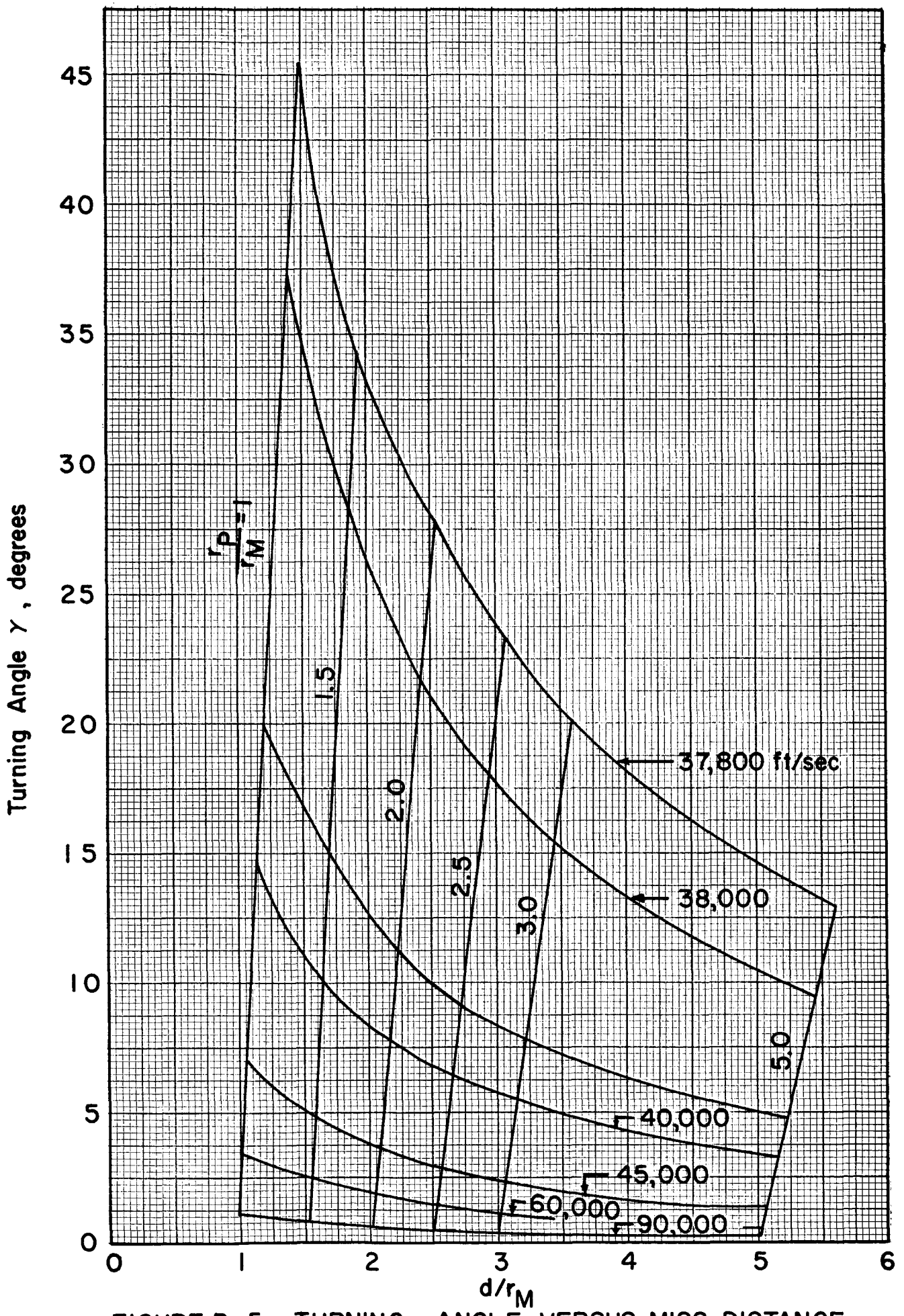

FIGURE B-5. TURNING ANGLE VERSUS MISS DISTANCE AT MARS

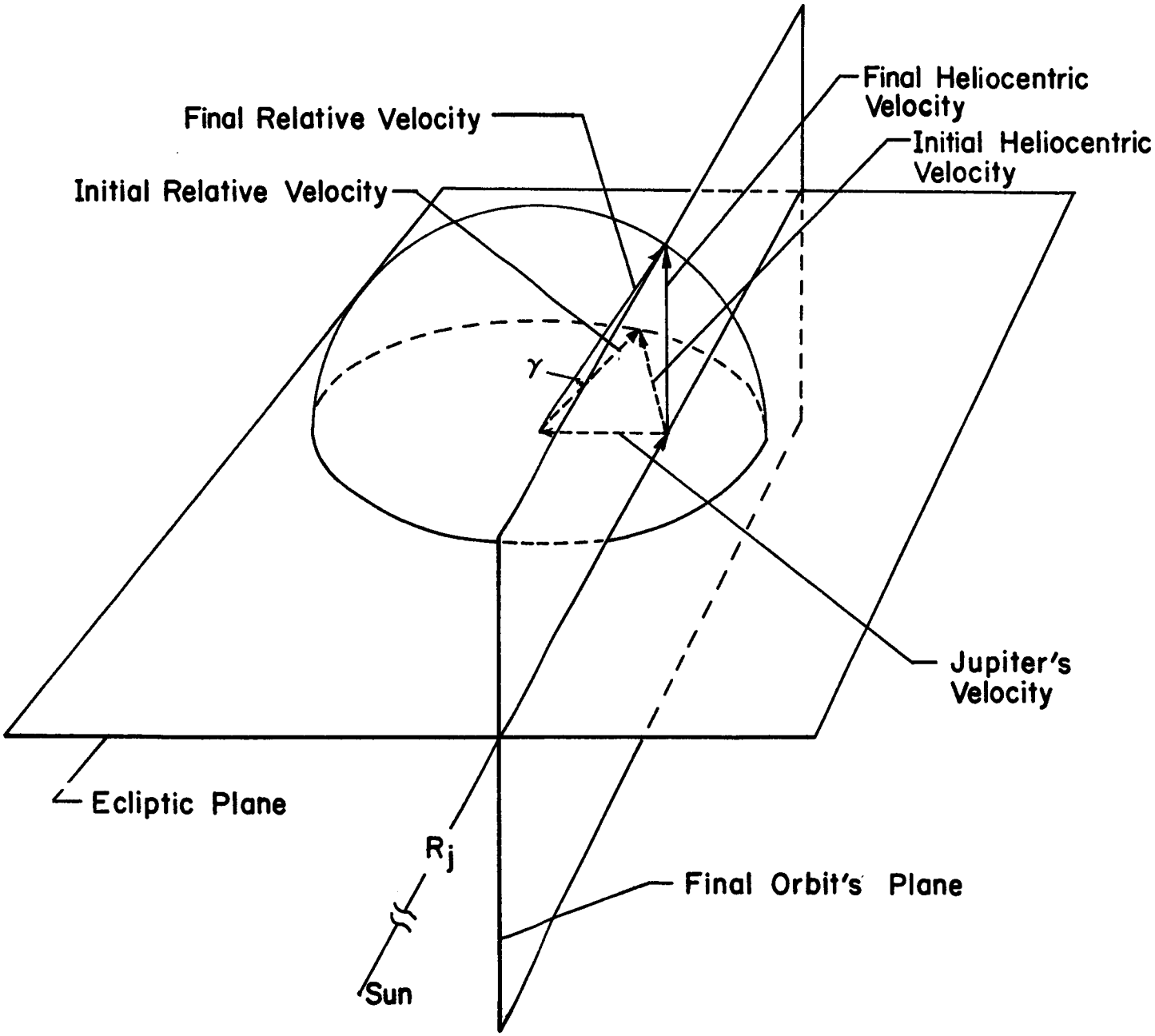

FIGURE B-6. VECTOR DIAGRAM OF ENCOUNTER FOR TYPE I ORBITS

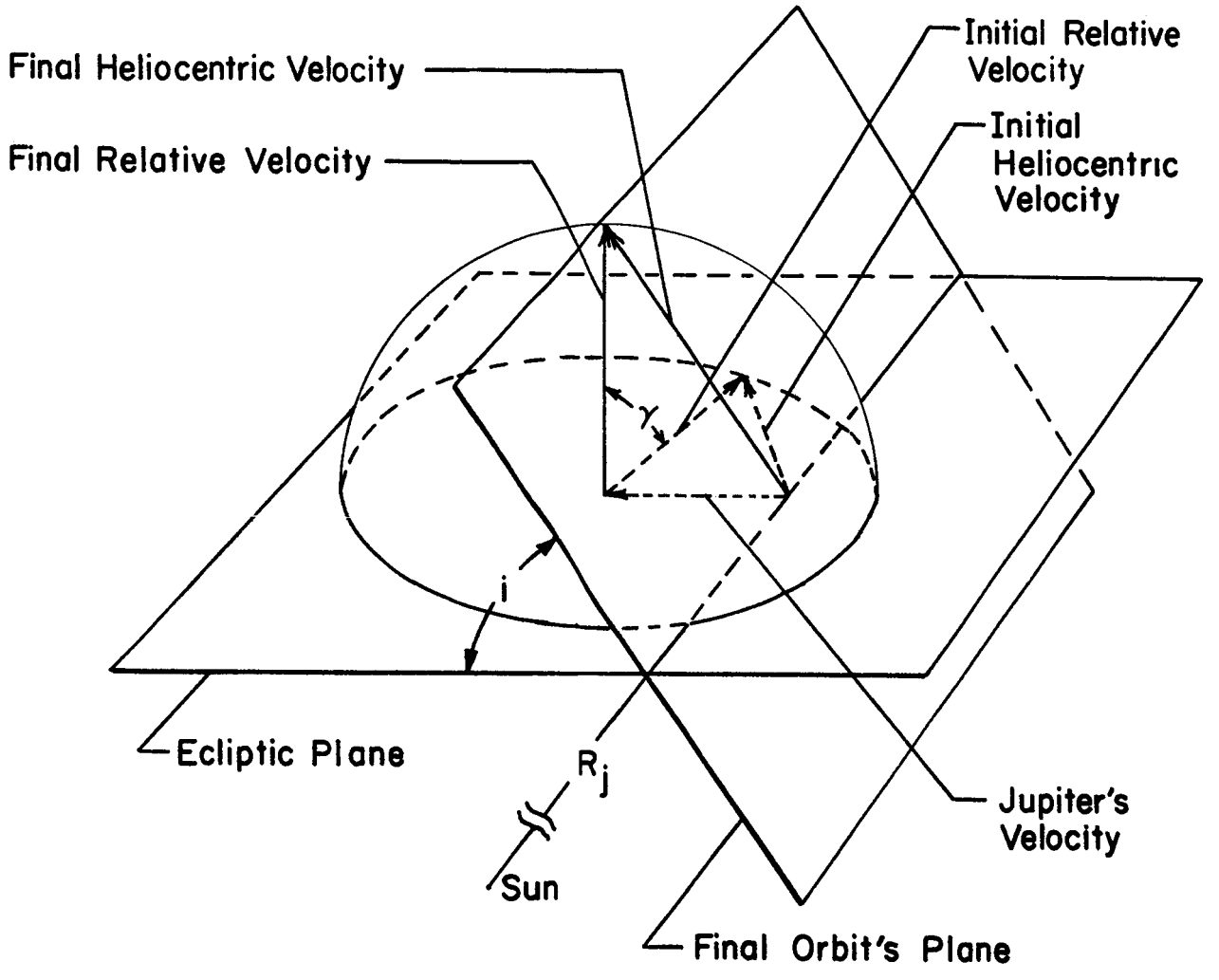

FIGURE B-7 VECTOR DIAGRAM OF ENCOUNTER FOR TYPE II ORBITS